AN EXPERIMENTAL INVESTIGATION OF FLOW CONDITIONS BEHIND A BLUFF BODY FLAMEHOLDER

Thesis by

Paul W. Utterback

Lieutenant, United States Navy

In Partial Fulfillment of the Requirements

For the Degree of

Aeronautical Engineer

California Institute of Technology

Pasadena, California

1960

ACKNOWLEDGMENTS

I wish to express my deepest appreciation to Dr. Edward E. Zukoski for suggesting this subject for investigation. Dr. Zukoski's interest and suggestions were highly instrumental in the conduction of this work.

To Dr. F. H. Wright, Project Engineer, Jet Propulsion Laboratory, I extend my gratitude for his interest and guidance throughout the experimental work and his comments on this manuscript. I also wish to thank Mr. James Creson for his assistance in reducing the data; Mr. Vernon Taylor, for his outstanding work in operating and maintaining the equipment; the Photographic and Report sections of the Jet Propulsion Laboratory for the excellent presentation of all figures; and Mrs. Roberta Duffy for her meticulous typing of this manuscript.

Appreciation is extended to the Bureau of Weapons, Department of the Navy, which has approved and supported this graduate work.

ABSTRACT

Carbon-containing combustion products were analyzed behind a bluff body flameholder in a two-dimensional duct. Molar concentrations of carbon monoxide, carbon dioxide, and unburned hydrocarbon fuel were obtained at various positions vertically across the duct 34 1/8 inches behind the flameholder by means of an Infra Red Analyzer. A carbon balance was conducted across the duct, and parameters such as combustion efficiency, temperature, pressure, sampling rate, density, and velocity of the gas mixture were determined.

The data indicate that the methods of sampling and measurement and the use of the analyzer were satisfactory in this type of investigation. Division of the flame into three distinct zones (unburned, reaction, and burned) is shown to be a reasonable approximation. The carbon balance across the duct was found to be in good agreement with theoretical predictions, provided that the water vapor in the gas samples was properly evaluated. Flame spreading behind the flameholder is a slow process, and this fact was verified by evaluation of the combustion efficiency and by determination of the limits of the burned zone.

TABLE OF CONTENTS

LIST OF TABLES

LIST OF FIGURES

LIST OF SYMBOLS

A	Cross-sectional area of sample probe
CH	Abbreviation for hydrocarbon fuel
CO	Carbon monoxide
CO_2	Carbon dioxide
C_p	Specific heat
M	Molecular weight
R	Universal gas constant
S	Cross-sectional area of the combustion duct
T	Temperature
VP	Vapor pressure of water
h	Local enthalpy
m	Weight
$\dot{m}$	Weight flow rate
n	Number of moles
p	Pressure
q	Dynamic pressure
Δ	Change in
η_c	Combustion efficiency
λ	Ratio of unburned gas density to burned gas density
ϕ	Fuel-air equivalence ratio, fraction of stoichiometric
ρ	Density

Subscripts

air	Standard air
CH	Hydrocarbon fuel
CO	Carbon monoxide

CO_2	Carbon dioxide
H_2O	Water
mix	Mixture
a	Adiabatic flame temperature
c	Carbon
o	Station upstream of flameholder
t	Total
x	Local station across the duct

I. INTRODUCTION

With the advent of high performance supersonic aircraft utilizing afterburning turbojet engines and air-breathing guided missiles using ramjet engines, it was necessary to provide means for continuous ignition of the fast-moving burnable gas mixtures. Such a flame stabilization process was achieved by placing bluff bodies of various shapes and sizes in the gas stream. The burned gases recirculating in the wake of the bluff body provide a continuous source of ignition for the high-velocity combustible mixture. Considerable research has been conducted in this field to determine the mechanism of flame stabilization and the important parameters of maintaining combustion.

Early experiments by Nicholson and Fields[1], Longwell[2], Haddock[3], and Scurlock[4, 5] demonstrated the practicability of flame stabilization in high velocity mixtures by the use of bluff bodies. A photograph of a flame stabilized on a circular cylinder flameholder is shown in Figure 1. This flame has two distinct regions; the recirculation zone directly behind the flameholder, and the propagating flame extending downstream from the recirculating region spreading into the unburned gas.

Zukoski[6] divided the recirculation region into two zones; recirculation and mixing. The recirculation zone consists of the area directly behind the flameholder where hot burned gases are continually recirculating. The mixing zone is a turbulent region on the perimeter of the recirculation zone in which the burned gases supply heat to the combustible mixture, causing ignition. This ignition process is continuous, providing there is sufficient heat transfer in this zone. This ignition process has been thoroughly studied and the processes of importance are understood.

The flameholder and accompanying recirculation zone act as an anchor for the spreading flame which slowly propagates into the unburned gas flow. Photographs show that far downstream from the flameholder, the flame appears as two distinct luminous bands separating two transparent zones. In this area the flame has been assumed to consist of three regions; unburned, reaction, and burned. The unburned zones are the external homogeneous areas in which chemical action has not occurred. The adjacent areas are the reaction zones which are easily identified by their luminous appearance. The central region is again not luminous, and is assumed to consist of burned gas. A gas element entering the reaction zone becomes a non-homogeneous mixture of burned, partially burned, and unburned gas, and remains in the zone until the element is almost completely burned. It then passes from the luminous area into the burned zone, which is the hot area composed of products of combustion.

The spreading rate of a flame of this configuration has been investigated by Thurston[7] and Satre[8]. The characteristics of the spreading process found in these studies may be summarized as follows: at speeds above a critical value, the reaction zone has a turbulent appearance in high speed schlieren photographs, and in this turbulent regime the flame spreading rate is substantially independent of approach stream speed, fuel-air ratio, and temperature. In addition, far downstream from the flameholder, turbulent flame rates are independent of flameholder geometry and scale. The reaction zone thickness was also found to be independent of the parameters discussed here. The present work was carried out to determine the flow parameters for a particular station downstream of the flameholder, with some generality, for the

turbulent flow regime. The chemical parameters measured were the concentrations of carbon monoxide, carbon dioxide, and the hydrocarbon fuel. The fluid dynamic parameters which were evaluated include the temperature, density, pressure, and velocity of the gas mixture. The summary of information concerning flame spreading presented in this paragraph indicates that the measurement of these quantities at a single station is of general interest.

A continuous flow method was used in this investigation to determine the chemical composition of combustion gases. Gas samples extracted from the combustion mixture passed through a Beckman Infra Red Analyzer where carbon-containing products were analyzed. Since the reaction zone and the central core were regions of non-homogeneity, particular care was used to withdraw samples at a flow rate equal to the local velocity.

II. EXPERIMENTAL APPARATUS

Figure 2 is the schematic diagram of the basic equipment and flow system used in this investigation. The apparatus included the air supply and control system, liquid fuel supply, ignition, temperature and pressure systems and the gas sample analysis system.

A well-regulated supply of air was heated to a fixed temperature in the heat exchanger system. The hydrocarbon fuel was injected into the heated air well upstream of the plenum chamber to ensure complete vaporization and to provide a homogeneous gas mixture at the plenum chamber. A smoothly converging nozzle connected the plenum chamber to the combustion duct. This ensured that a uniform flow having low turbulence, fixed temperature, and controlled velocity, would enter the combustion chamber.

Air Supply and Control System

The air supply was furnished by two reciprocating pumps with a capacity of 3.7 lbs/sec at a pressure of 100 psig. The mass flow rate was regulated by a remotely controlled sonic-throat regulating valve located upstream of the heat exchanger and fuel injector. In this manner, the air mass flow rate was made independent of variations in mixture temperature, fuel injection rate, or fuel-air ratio, and combustion chamber conditions. Mass flow was measured downstream of the heat exchanger and upstream of fuel injection by use of a sharp-edged orifice. The flowmeter used both mercury and water manometers for measuring pressures, and a chromel-alumel thermocouple read by a Brown Automatic Potentiometer was used in measuring temperature. A constant air

mass flow rate was maintained on all runs in this investigation, since it was desired to create similar conditions on all runs.

Air Temperature Control

The mixture temperature was maintained by passing a portion of the incoming air supply through a multitube heat exchanger. A turbojet can burner with an independent air supply was used as a heat source. Two butterfly valves fixed the portion of air passing through the heat exchanger. The operation of these valves or regulation of the fuel to the turbojet can burner could be used to maintain the desired mixture temperature entering the combustion duct. With this system, the temperature was controlled within $\pm$ 2°C for long periods of operation regardless of flow rates or mixture ratios.

In this investigation, it was desired to eliminate mixture temperature as a variable. Therefore, in all experimental runs the temperature was maintained as constant as possible at 100°C. This temperature was chosen since it was high enough to ensure complete vaporization of all fuel components.

Fuel System

The fuel used was Standard Oil Thinner No. 200, whose detailed specifications are given in Table A. This gasoline-type fuel was used because of its uniform chemical properties, availability, ease of handling and metering. Fuel tanks of 600-pound capacity were pressurized to 150 psig with nitrogen pressure bottles. Fuel was injected into the air supply through a constant-pressure, variable-area nozzle well upstream of the plenum chamber to ensure proper vaporization. The fuel was metered by

a Fisher-Porter Flowrater which measured the flow within $\pm \frac{1}{2}$ lb/hr.

In this investigation, fuel-air mixture was eliminated as a variable. In all runs, the fuel flow was maintained as constant as possible at 400 lbs/hr. This flow rate gave a calculated fuel-air equivalence ratio of $\phi = .93$.

Ignition System

The ignition of the fuel-air mixture in the duct was accomplished by a high-voltage spark between a remotely positioned igniter rod and the surface of the flameholder. A 4,000 volt power supply provided sufficient power to produce ignition for the flow velocities used in this investigation.

Plenum Chamber and Nozzle

The plenum chamber (see Figure 2) was a 24-inch diameter cylinder 90 inches long. The high speed fuel-air mixture entering the chamber was broken up by three perforated blockage plates at the upstream end of the chamber. The circular cross-section of the chamber was converted into a 15-inch square cross-section 15 inches after the first blockage plate. Two 30-mesh and two 60-mesh wire screens were mounted in the downstream end of the plenum chamber to reduce the turbulence of the mixture entering the nozzle. An 8-inch rupture disk was provided in the top of the plenum chamber at the upstream end to allow quick reduction in plenum chamber pressure in the event of a blow back. Also, a flame arrester was placed just upstream of the chamber to prevent flashback through the lines.

A 15-inch convergent nozzle reduced the cross-section from the 15-inch square cross-section to the 3" x 6" rectangular cross-section of

the combustion duct, giving a contraction ratio of 12.5:1. Pressure surveys of the inlet to the combustion duct showed a flat velocity profile.

Combustion Chamber and Flameholder

The combustion chamber was a 3-inch by 6-inch rectangular duct 33 1/2 inches long (see Figures 3 and 4). The side walls were made of six 6 7/16-inch high by 5 9/16-inch wide Vycor glass plates. The plates were inscribed at every inch with straight lines parallel to the duct axis to facilitate accurate location of pressure and gas sampling probes in the duct. The forward ends of the glass plates were supported by 1-inch wide cold-rolled mild steel plates. These plates also served as the mounting plates for the 1/4-inch circular cylinder flameholder. The glass plates allowed visual and photographic observation of the flow. The top and bottom walls of the duct were made of stainless steel. These plates were water-cooled to prevent warpage of the duct.

A 1/4-inch circular cylinder water-cooled flameholder was used during this investigation. It was constructed of stainless steel tubing and located on the centerline at the upstream end of the duct. The water cooling maintained the temperature of the flameholder constant throughout the tests.

Pressure and Temperature Measuring Equipment

The plenum chamber total pressure, the combustion chamber entrance static pressure, and the pressure difference were measured by both water and mercury manometers. The plenum chamber total head was obtained from a total head probe located on the vertical centerline just upstream of the nozzle. A series of six static pressure taps located

5 inches upstream of the flameholder was led to a common line to obtain the average static pressure reading at the combustion chamber entrance. The sampling probe was also used to measure total pressure in the flame.

The inlet mixture temperature was measured in the plenum chamber with a chromel-alumel thermocouple. The thermocouple voltage readings were measured with a Brown Automatic Potentiometer.

Gas Sampling Equipment

Gas samples were taken at various stations across the duct by use of water-cooled sampling probes of two sizes; .0135" by .079" elliptical probe, and a .050" inside diameter probe. The probes were constructed of stainless steel, and were water-cooled to prevent burning of the probe tips and to ensure adequate quenching of the samples. Tips of the probes extended beyond the water-cooled jacket to prevent interference. Samples withdrawn from the stream were passed through a 1/4-inch copper tube to an infrared analyzer, to a flow meter, and finally to a vacuum pump. Pressure in the sampling tube was measured by use of a mercury manometer. While the samples were withdrawn, a partial vacuum of three-tenths of local atmospheric pressure (730 mm Hg) and an average room temperature of 22°C were maintained at the entrance of the gas analyzer. Flow rate was adjusted by a valve, which allowed the sample rate to be varied through the desired range. A Fisher-Porter Flowmeter was used and calibrated to measure the flow in gms/sec. The instrument had an accuracy of $\pm$ .001 gms/sec.

The probes were mounted to permit vertical and fore-and-aft movement. Vertical probe positioning was accomplished by a remote-control electric motor and indicator whereby the probe could be positioned

within $\pm$ .001 inch. Position calibration was accomplished by use of the scribes on the Vycor glass plates. Due to turbulence in the wake and heating of the probe, some wandering of the probe occurred during a series of tests. Repeated tests were made of probe zero positions and gas analyzer data to ensure experimental accuracy.

A Beckman Infra Red Analyzer was used to measure gas components of hydrocarbons, CO and CO_2. Samples withdrawn from the combustion duct were investigated at a partial pressure of three-tenths atmosphere and a temperature of 22°C. The analyzer was calibrated against samples of hydrocarbon, CO, and CO_2 of known composition. Hydrocarbon readings were corrected for CO and CO_2 cross contamination, since these components gave small increases in the hydrocarbon reading, depending on their concentration. The analyzer was calibrated to read molar fraction of the component in the test sample. Readings were measured in milliamperes and converted to molar fraction by use of calibration curves, obtained from tests with samples of known composition.

Combustion duct temperature surveys were conducted using the sodium line reversal method and chromel-alumel thermocouples. In the line reversal method, a 6-volt tungsten lamp was calibrated for brightness temperature by use of a standard pyrometer. The lamp was calibrated after each run. Sodium chloride and sodium nitrite were used to introduce sodium into the flow; they were placed in the duct 10 inches upstream of the station being investigated by use of a streamlined, perforated pinched probe. The probe was inserted in the flame just long enough for a reliable reading and then removed to prevent burning of the probe.

Schlieren Equipment

A conventional double-mirror type schlieren system with a BH-6 mercury vapor light source was used. The mirrors were concave, 10 inches in diameter, with focal lengths of 78 and 85 inches respectively. A flash system with a flash duration of approximately 7 microseconds was synchronized with the camera shutter by timing relays. A short spark duration was used to stop motion. Super XX film was used for all photographs.

III. EXPERIMENTAL PROCEDURE

All results and data were taken from a station 34 1/8 inches behind the flameholder, as shown in Figure 3. This station is just outside the duct.

In this investigation, all runs were performed under the same operating conditions. This was done by maintaining a constant air mass flow rate, a constant fuel injection rate, and a plenum exit temperature of 100°C. The measured fuel-air ratio was 0.063, which gave an equivalence ratio of 0.93; and the Mach number was 0.20. The flame was turbulent, and combustion chamber oscillations were negligible. Corrections for variations in local atmospheric pressure and temperature, plenum temperature, and fuel-air ratio were taken into account in evaluating the results.

Sample Extraction Rate

In order to have a valid evaluation of mixture composition, it is necessary to extract the sample from the duct at a velocity corresponding to the velocity of the mixture at that point. Sample extraction rates greater than local velocity produce a mixture with a greater proportion of lighter density components, and slower rates produce an excess of the more dense components. Experimental results, e.g. reference 9, support this statement. Also, Leeper, in reference 10, indicates that oscillations may be set up in the sampling probe due to an incorrect sampling extraction rate, which would produce further errors in the component proportions in the mixture.

The length of the probe extending beyond the water-cooling jacket

was regulated to meet two conditions. If the probe were too short, then interference would be created by the probe water-cooling jacket, and if the probe were too long, it would become overheated and possibly fail or become clogged. Also, in a hot probe, reaction of the mixture would continue to occur, giving erroneous results for gas composition at that station. A probe length of less than one inch was used to ensure proper cooling and quenching of the samples and to eliminate most of the cooling jacket interference.

Two sizes of probes were used. The .0135 by .079-inch elliptical probe was used in the outer portion of the duct where high sampling rates and moderately low temperatures were encountered. In the inner region, where the temperature approached the adiabatic flame temperature, this probe failed due to insufficient cooling, and samples were improperly quenched. In this central portion of the duct, the .050-inch probe was used, where low sampling rates and high temperatures were encountered. This probe was constructed of heavier tubing than the elliptical probe and was 1/8" shorter, which gave it better heat transfer characteristics. Pressure losses in the sampling tubes connecting the probe to the vacuum pump, and insufficient capacity of the vacuum pump, precluded the use of the larger sampling probe, i.e., the 0.050-inch probe, in the outer regions of the duct where high sampling rates were required.

The correct sampling rate was determined by use of the mass flow equation:

$$\dot{m} = \rho V A \quad .$$

The area of the probe was accurately determined from direct measurements and was corrected for thermal expansion.

In order to obtain ρ and V, a more complicated procedure was necessary. The molecular weight of the gas mixture at all conditions of partial combustion was required. Curves showing the ratio of the molecular weight of Standard Oil Thinner No. 200 to the molecular weight of air as a function of percentage of mixture burned for various values of equivalence ratio, ϕ, have been prepared by Dr. F. H. Wright[11]. Dr. Wright calculated the properties of the mixture, taking into account the appropriate fractions of combustion products and unburned gases. Decomposition of the fuel into lighter hydrocarbons was neglected. This decomposition of fuel in the real case would not make appreciable errors, since the fuel-air ratio, 0.063, is small.

The percent of CO_2 measured at a station at a particular sampling rate could be used to obtain an approximation for the local combustion efficiency. From this approximation, the molecular weight ratio, (M_{mix}/M_{air}), of the partially burned mixture can be estimated. Assuming the mixture acts as a perfect gas at these elevated temperatures, the universal gas law was considered valid:

$$p = \frac{\rho R T}{M}$$

Therefore:

$$\rho_{mix} = \frac{p_{mix} M_{mix}}{R T_{mix}} \quad , \text{ and } \quad \rho_{air} = \frac{p_{air} M_{air}}{R T_{air}} \quad ,$$

where ρ_{air} is evaluated at 100°C and 730 mm Hg = 5.68×10^{-2} lbs/cu ft.

The local temperature still must be measured before ρ_{mix} can be evaluated. The temperature across the duct was determined by the sodium line reversal method and by chromel-alumel thermocouples. The line reversal method was used in the center region of the duct where the tem-

perature approached the adiabatic flame temperature. This method measures the local static temperature of sodium gas in terms of the brightness temperature of a tungsten filament which must be converted to true temperature.

The thermocouple was used in the outside regions of the duct where the temperature was not as high. Corrections for conduction and radiation losses were made, using reference 12, to give total temperature, which in turn was converted to static temperature. At the Mach numbers used in this experiment, the difference between static and total temperature was less than 2 per cent.

The static pressure across the duct has been shown to be constant, and is equal to the local atmospheric pressure at the station used.

Therefore, using these measured values of p_{mix}, T_{mix}, and the approximate value of (M_{mix}/M_{air}), the density ρ_{mix} can be determined:

$$\rho_{mix} = \frac{\rho_{air} T_{air}}{T_{mix}} \left(\frac{M_{mix}}{M_{air}} \right) = \frac{2.12}{T_{mix}} \left(\frac{M_{mix}}{M_{air}} \right) .$$

The same results could be determined by finding M_{mix} and placing this value in the universal gas law; however, the above relationship compares the gas density with air at 730 mm Hg and 100°C, which is more convenient.

As a check, the molecular weight ratio was verified by comparing with curves of (M_{mix}/M_{air}) vs. temperature found in reference 11.

The velocity was determined using Bernoulli's equation for steady flow and the universal gas law:

$$V = \sqrt{\frac{2 (p_t - p)_{mix}}{\rho_{mix}}} ,$$

where all values of the parameters have been previously determined.

The equations can thus be summed as:

$$\dot{m} = \rho V A = A\sqrt{2\rho_{mix}(P_t - P_{mix})} = A\sqrt{\frac{4.24\,\rho_{mix}}{T_{mix}}\,\frac{M_{mix}}{M_{air}}\,(P_t - P)_{mix}}.$$

Using the sampling rates determined by the above relationship, better values of CO_2 percentage were found, which then led to a better approximation for sampling rates. Thus, by a reiteration process, which was convergent, the correct sampling rates were calculated. With these determined sampling rates, CO_2, CO, and hydrocarbon molar concentration surveys were conducted. Concentrations at sampling rates below and above the correct rate were also determined to investigate the change of component concentration with sampling rate.

A cross-plot of probe total pressure vs. stations across the duct was used in conjunction with the probe position indicator to ensure positioning of the probe in the same spot in the duct on various runs.

Gas Analysis of Combustion Products

One of the parameters of interest is the total carbon balance. The carbon balance at all stations across the duct was determined by comparing the total amount of carbon in the mixture sample with the amount of carbon in the unburned mixture. The carbon-containing components in the mixture sample were the unburned hydrocarbon fuel, CO_2, and CO. The molar fractions of the components were determined by use of the Infra Red Analyzer.

It was necessary to correct these data for loss of water vapor from the sample. Two assumptions concerning the condition of the sam-

ple at the analyzer were used in reducing the data; first, that the gas sample was at most saturated; and second, that the gas sample was dry. The corrections were based first on the measured value of the local combustion efficiency and second on the stoichiometric equation for complete combustion for $\phi = 0.93$.

$$.93\ C_{6.822}H_{13.955} + 10.31\ O_2 + 38.85\ N_2 =$$

$$6.34\ H_2O + 6.49\ CO_2 + .72\ O_2 + 38.85\ N_2$$

The combustion efficiency determines the total moles of combustion products (n_t) and the moles of H_2O formed (n_{H_2O}). In the partially burned mixture there are also present quantities of H, H_2, NO, OH, O, and CO. These species appear in very minute amounts until the mixture approaches complete combustion, when the temperature approaches the adiabatic flame temperature, and dissociation occurs. Even under these conditions, CO equilibrium concentration is 0.75 per cent and the total of the remaining components is less than 0.82 per cent. Thus, the total concentration of this group is small compared to the assumed products of complete combustion, and may be neglected.

The partial pressure of water vapor in the mixture is the total pressure of the mixture times the ratio of the number of moles of water vapor to the total number of moles of combustion products:

$$P_{H_2O} = \left(\frac{n_{H_2O}}{n_t}\right) \cdot P_{mix}$$

where the pressure of the sample during analysis, $P_{mix} = 219$ mm Hg. A sample temperature of 22°C gave a vapor pressure, VP_{H_2O}, of 19.827 mm Hg.

For the first assumption, when the partial pressure of the water vapor in the mixture exceeds the vapor pressure of water at a given temperature, water is assumed to condense. The amount of water condensing is:

$$\left(\frac{P_{H_2O} - VP_{H_2O}}{P_{H_2O}}\right) \quad n_{H_2O}$$

The molar concentration of any component can be determined by adjusting for this loss. The corrected molar concentration for the first assumption is:

$$\left(\frac{n_x}{n_{mix}}\right)_{cor.} = \frac{n_x}{n_{mix}}\left(1 - \frac{n_{H_2O}}{n_t}\left[\frac{P_{H_2O} - VP_{H_2O}}{P_{H_2O}}\right]\right) .$$

The corrected concentrations were then reduced to gms of carbon per mole of mixture:

$$m_{fuel} = \left(\frac{n_{fuel}}{n_{mix}}\right) M_{fuel} \quad \text{in gms/mole mixture}$$

where n = number of moles and M = molecular weight.

For Standard Oil Thinner No. 200, M = 96, chemical formula $\doteq C_{6.822}H_{13.955}$, and for $\phi = 0.93$. The amount of fuel in the theoretical unburned mixture is:

$$m_{fuel} = .018536 \times 96 = 1.781 \text{ gms fuel/mole mixture} .$$

The amount of carbon in the unburned mixture is:

$$m_{C_{fuel}} = .018536 \times 6.822 \times 12.01 = 1.519 \text{ gms carbon/mole mixture} .$$

Similarly, the amount of carbon due to the hydrocarbons in a mixture sample is:

$$m_{c_{CH}} = \left(\frac{n_{CH}}{n_{mix}}\right) \times 6.822 \times 12.01 = 81.93 \left(\frac{n_{CH}}{n_{mix}}\right) \text{ gms carbon/mole mixture.}$$

The carbon in the CO_2 is:

$$m_{c_{CO_2}} = \left(\frac{n_{CO_2}}{n_{mix}}\right) \times 12.01 \text{ gms carbon/mole mixture .}$$

The carbon in the CO is:

$$m_{c_{CO}} = \left(\frac{n_{CO}}{n_{mix}}\right) \times 12.01 \text{ gms carbon/mole mixture .}$$

The total grams of carbon per mole of mixture at any station, x , is found by adding the carbon contributions of the unburned hydrocarbons, CO_2, and CO:

$$m_{ct_{(x)}} = m_{c_{H_2O_{(x)}}} + m_{c_{CO2(x)}} + m_{c_{CO_{(x)}}}$$

As shown in reference 11, molecular weight of the mixture decreased as the mixture burned to completion. Dividing $m_{ct_{(x)}}$ by the corresponding molecular weight which was discussed earlier, the ratio [(gms of carbon)/(gms of mixture)] was determined. Dividing this quantity by [(gms of carbon)/(gms of mixture)] of the unburned mixture gives a normalized carbon balance for each station.

The second method of obtaining the carbon balance was based on the assumption that all water vapor was removed from the samples. The corrected molar concentration then is

$$\left(\frac{n_x}{n_{mix}}\right)_{cor.} = \frac{n_x}{n_{mix}} \left(1 - \frac{n_{H_2O}}{n_t}\right) .$$

The corrected concentrations were then normalized as described above.

IV. DISCUSSION OF RESULTS

General

The time exposure photograph, Figure 5, shows the three distinct zones in the duct. In the outside region, the gas mixture is unburned. The region of strong radiation is the reaction zone, in which the gas consists of a mixture of unburned, partially burned, and burned materials. The central portion of the wake which appears dark is a region of burned, and hence non-radiating, gas. In a schlieren photograph, Figure 6, the unburned region is uniform; the reaction zone shows large gradients substantiating the presence of chemical reaction and mixing. The burned region appears as a transparent region, and is reasonably free of striations, indicating that this region is composed primarily of completely burned gas. References 6 and 7 go into further detail in the discussion and photographic interpretation of these regions.

Examination of photographs such as Figures 5 and 6 and the tabulated data show that the reaction zone extended from + 1.0 to + 2.0 inches above the centerline, and - 0.8 to - 1.8 inches below the centerline at the 34 1/8-inch station. This indicates the combustion profile is slightly unsymmetrical about the centerline of the duct, the center being at + 0.1 inches. Investigation of the Vycor glass plates at the conclusion of the investigation revealed some warpage due to the intense heat in the burned region. This warpage and the comparatively long distance downstream from the flameholder makes this slight shift in the centerline quite feasible. Although the flame is in a gravity field, convection would shift the flame profile upwards less than 0.02 inches.

Total Pressure Survey

The total pressure survey in Figure 7 shows a constant pressure in the unburned region outside of the boundary layers, and a marked decrease through the reaction zone, and then a gradual increase to the centerline. Passing through a simple laminar flame front, a gas element undergoes a large density change and a negligible change in velocity. Hence, the change in total pressure, Δp_t, is the result of the change in dynamic pressure and can be expressed by

$$\Delta p_t = q_x \left(1 - \frac{1}{\lambda}\right)$$

where q_x is the local dynamic pressure, and λ is the ratio of the unburned gas density to the burned gas density. Since λ is of the order of 6, the total pressure loss due to combustion alone is of the order of 0.85 q_x for simple systems. In the present case, an additional loss due to mixing is to be expected. The observed change is about equal to 1.0 q_x, which agrees well with the predictions.

The rise of total pressure within the burned region can be accounted for by investigating the previous history of the gas elements. A gas element on the centerline entered the burned region furthest upstream where the velocity and dynamic pressure were lower. Therefore, it is expected that the total pressure will be slightly higher as the center of the unburned region is reached.

Temperature Profile

A plot of the temperature profile across the duct is shown in Figure 8. In the center region, the sodium line reversal method was used. Sodium injected into a burned gas is vaporized and its temperature is raised to that of the gas. It is the temperature of the sodium vapor in the

gas mixture which is measured in the line reversal method, and this is an indication of gas temperature. In a mixture of burned and unburned gas, only the burned portion of the gas would vaporize the sodium, and the line reversal method would be measuring the temperature of the burned gas and not the average value for the complete mixture. Thus, the peak temperature and not the average temperature is measured. In the burned zone of the flame (e. g. see Figure 10), where combustion is nearly completed and the gas is nearly homogeneous, the line reversal method gives an accurate value for the mixture temperature. The peak temperature in the duct was 2135°K, or 5. 5 per cent below the theoretical value of the adiabatic flame temperature of 2250°K. Two reasons for this difference can be cited. Complete combustion was not attained at the centerline; and sodium was injected into the duct in an aqueous solution and heat was removed from the gas to vaporize and heat the solution. Radiation and convection losses are negligible, since the speeds used in the duct were above 247 ft/sec and the stay time of a gas element in the duct was of the order of 8 milliseconds. In the reaction zone, the amount of unburned gas to burned gas became appreciable, and the line reversal method measured the burned gas temperature rather than the mixture temperature. This accounts for the high line reversal results in this zone.

Starting in the unburned zone, thermocouple readings were taken until the thermal limits of the thermocouple were reached. The thermocouple reads the average total temperature at any station. Unlike the line reversal method, it does not distinguish between burned and unburned gas temperature, but records the mass average.

Extrapolation of the thermocouple data intercepted the sodium line

points at the inside limits of the reaction zone. The combination of these two sets of data gives a reasonable temperature profile.

Gas Density Distribution

Figure 9 displays the gas mixture density distribution across the duct. These data were based on the measured temperature profile. The density decreases rapidly through the reaction zone and then stabilizes in the burned zone. This leveling in the central region substantiates the assumption that the burned zone is composed primarily of completely burned gas. Both the pressure and density profiles show clearly the slight shift in centerline as previously discussed.

Velocity Distribution

Figure 11 depicts the velocity distribution across the duct. The curve shows a steep velocity gradient through the reaction zone, which is the result of the high density gradient in this region. In the burned zone, where the gas density is almost constant, the velocity gradient is less and is a result of the increase in total pressure. It appears that the velocity may be approximated by a linear variation from the edge of the flame to the centerline without incurring appreciable errors.

Sample Extraction Rate

Using the velocity and density distribution, the ideal sample extraction rate was determined, and is displayed in Figure 12. It is of interest to note that in the reaction zone, the rate of decrease in gas density predominated and produced a decrease in the sampling rate. In the burned region, the velocity became the predominant factor since the density approached a constant value, and the ideal sample rate increased.

At several stations across the duct, two sizes of sample extraction probes were used. The variation of sample concentration due to probe size was negligible, as shown in Figure 13.

It is evident from Figure 13 that the hydrocarbon concentration is slightly sensitive to the sampling rate. A change in rate from 3.5 gms/sec to 10.5 gms/sec produces a variation in hydrocarbon concentration of 5 per cent. Figure 12 shows a required change in sampling rate of more than a factor of 3 when centerline and unburned sampling rates are compared. Thus the extreme importance of using the correct sampling rate is demonstrated. The same observation equally applies to the variation of CO, CO_2, and hydrocarbon concentrations with sampling rate at other positions in the flame.

The variations of species concentrations with sampling rate is a maximum in the reaction zone, and drops off as the centerline is approached. This indicates that the gas is a non-homogeneous mixture in the reaction zone and approaches homogeneity in the burned zone.

Component Concentration Curves

Figures 14, 15, and 16 show the uncorrected molar per cent concentration of CO, CO_2, and unburned hydrocarbons across the duct at the proper sample extraction rate.

Figure 14 shows that CO concentration reaches a peak near the inside edge of the reaction zone and then decreases as the centerline is approached. In the reaction zone, the combustion does not go to completion and excess CO is formed. The time for a gas element to pass through the reaction zone is of the same order as that for a gas element passing through a laminar flame, i.e., about 5 to 10 milliseconds.

During this time, chemical reaction has been initiated, but chemical equilibrium has not been reached; and the excess CO has not reacted with the remaining oxygen to form CO_2.

The sample entering the extraction probe is quenched by the probe water-cooling jacket in a distance of one inch; at the velocities observed in this investigation, this would give an approximate quenching time of 0.2 milliseconds. This time is short enough to prevent equilibrium from being reached, and the excess CO is frozen in the sample.

As the centerline is approached, total combustion and equilibrium are approached. The CO molar concentration reaches a minimum value of .763 per cent. This compares very favorably with the theoretical concentration of 0.752 per cent for equilibrium.

The CO_2 concentration indicates a continual increase in concentration with the greatest gradients occurring within the reaction zone. Near the center, there is a leveling off as the CO_2 approaches a maximum molar concentration of 12.29 per cent. This is slightly high when compared with the theoretical value of 11.31 per cent.

The hydrocarbon curve shows the same steep gradient in the reaction zone and leveling off in the burned zone. Of the three components measured in this investigation, the hydrocarbon was the most difficult to measure. An error in hydrocarbon concentration creates an error in overall carbon balance 6.8 times as large as the same error in CO_2 or CO. The hydrocarbons in the samples had a tendency to adhere to the walls in the infrared analyzer and the sample extraction tubing, and thus created a contamination problem. To reduce this to a minimum, the analyzer was flushed with nitrogen and evacuated until correct zero read-

ings were obtained. The extraction tubing was flushed with dried air. Near the centerline, where the actual hydrocarbon concentration was quite small, even the slightest amount of contamination would create an appreciable error. It is believed that this was the predominant reason for the flattening of the curve at the centerline instead of approaching a zero concentration as expected. It was possible to make corrections for the effects of CO_2 and CO concentration on the infrared analyzer hydrocarbon readings and for the hydrocarbon content in the air entering the combustion duct from the air compressors. However, these corrections had little effect on the results.

Note that the concentrations presented in Figures 14, 15, and 16 have not been corrected for any loss of water vapor.

Carbon Balance

There are strong indications that water vapor was absent from the gas samples entering the analyzer. Comparison samples extracted from the combustion duct were passed through a dryer prior to entry to the analyzer. Comparison of these results with samples passed directly through the analyzer showed no change in CO_2 concentration. If water vapor were present in the sample, the dried sample would have shown a richer concentration of CO_2. It appears logical to assume that the water condensed out of the sample and adhered to the walls of the sample extraction tubing between the duct and the analyzer. Purging of the sample tubing with dried air as described earlier would prevent the accumulation of water in the lines.

Figures 17 and 18 show the variation of the normalized concentrations of CO and CO_2, (gms carbon in species)/(gms carbon in unburned

mixture), as a function of position across the duct. The corresponding hydrocarbon curve and the complete hydrocarbon balance curve are shown in Figure 19. These figures are based on the assumption of a dry sample, and the data are normalized by the measured carbon content of the unburned mixture entering the combustion duct. In Figure 19, there is a discrepancy of 3.0 per cent with the theoretical value in the unburned region. Slight errors in the measurement of the fuel flow and air flow into the duct could account for some of this error. It is therefore considered more consistent to compare the carbon balance across the duct with the measured value of the carbon in the unburned mixture than to use the values obtained from air and fuel flow rate measurements.

Figure 19 shows that the greatest error was about 5 per cent high and that it occurred in the reaction zone; in the burned zone, the measurement was consistently lower than the expected value of unity. This suggests that there is diffusion of CO_2 from the burned zone, where CO_2 concentration is high, into the reaction zone, where the CO_2 concentration is relatively low. However, this suggested diffusion process is not important in fixing the overall carbon balance, and the accuracy of the methods used in this investigation is not high enough to show with confidence that diffusion actually occurs. Integration of the area under the carbon balance curve indicates the carbon balance for the entire duct is 0.995 of the total carbon balance of the unburned mixture across the duct.

The assumption of a dry sample lowers the normalized carbon balance on the centerline to 0.992 and causes the CO_2 and CO concentrations at the centerline to compare favorably with the theoretical values for complete combustion. It also lowers the hydrocarbon concentration

by 12 per cent on the centerline. The trends in the CO, CO_2, and hydrocarbon curves are unchanged by making the assumption of a dry sample. Hence, the conclusions drawn from Figures 14, 15, and 16 are still valid.

Figure 20 depicts the same carbon balance based on the assumption that the gas sample entering the analyzer is saturated with water vapor, and that the remaining water vapor has condensed and adhered to the walls of the sample extraction tubing. Errors of 11.5 per cent are encountered in the reaction zone, and an average error of 7 per cent in the burned region.

Comparison of Figures 19 and 20 readily shows the difference in carbon balance which can be encountered, depending upon the evaluation of the water vapor in the gas mixture. For the particular apparatus used in this experiment, the correct water vapor content lies between the dry and saturated levels, and lies closer to the dry sample assumption. A desiccator was not used in the investigation, since it had the tendency to remove hydrocarbons from the mixture when hydrocarbon concentration was high. A possible method of preventing the loss of water vapor would be the heating of the sample tubing. Time limitations prevented the investigation of this method.

Investigation showed that the carbon balance was very insensitive to changes in temperature. Taking a station in the center of the reaction zone, the local temperature was varied by 25 per cent. This variation caused a maximum change in sample extraction rate of 15.5 per cent, but a change in carbon balance of 0.3 per cent, as is shown in Table B. This station, used for example purposes, was 1.4 inches above the centerline, as in this region the change in molar concentration with sample extraction

rate of the three components was a maximum as shown in Figure 21. These curves show that the unburned hydrocarbons in the high density, unburned gas decrease in concentration with an increase in sample extraction rate, and the CO_2 and CO occurring in the low density burned gas increase with increase in extraction rate. This variation is in agreement with theory (e. g. see reference 9). Over the extraction rate range in the investigation, the carbon balance at any station varied very little. Thus, any error incurred in the previously mentioned method of determining the temperature profile had insignificant effects on the overall carbon balance.

Note that although the carbon balance is insensitive to the sampling rate, the species concentration does change strongly with sample extraction rate. This variation again supports the contention mentioned earlier that the gas in the reaction zone is a non-homogeneous mixture of burned, partially burned, and unburned gases, and once again shows the great importance of using the correct sample extraction rate.

Combustion Efficiency

An estimate of the total combustion efficiency at the station under investigation was calculated. The product of the density and velocity at each station across the duct was divided by the product of the unburned mixture density and velocity entering the combustion duct. A plot of this relationship is shown in Figure 22. This curve shows an approximate linear decrease in the reaction zone and a constant value in the burned zone. Integrating the area under this curve showed the mass flow rate passing the station under discussion was 1. 002 times as large as the mass flow entering the combustion duct.

Compressibility and boundary layer effects were ignored in this determination. Since both would tend to decrease this value slightly, the closeness in the evaluation is considered surprising.

Local combustion efficiency was calculated in two manners for comparison of results as shown in Figure 10. One method was based on the comparison of the CO_2 concentration at any station with the CO_2 concentration for the completely burned mixture:

$$\eta_{c_x} = \frac{n_{CO_{2(x)}}}{n_{CO_{2(a)}}}$$

The other method was based on the enthalpy change:

$$\eta_{c_x} = \frac{h_x - h_o}{h_a - h_o} = \frac{C_{p_x} T_x - C_{p_o} T_o}{C_{p_a} T_a - C_{p_o} T_o} \quad ,$$

where h is the local enthalpy, C_p the specific heat, T the temperature. The subscript, x, denotes the conditions at the local duct station; o, at the entrance to the duct; and a, at the adiabatic flame temperature. Specific heats were determined from reference 11, taking into account specific heat dependence on temperature for Standard Oil Thinner No. 200.

The total combustion efficiency was determined by multiplying the local combustion efficiency by the corresponding local mass flow rate ratio and integrating the area under the curve:

$$\eta_c = \int_o^{S_o} \frac{\eta_{c_x} \rho_x V_x}{\rho_o V_o} \, dS \quad ,$$

where S is the element of cross-sectional area and S_o is the total duct cross-sectional area.

A curve of

$$\eta_{c_x} \frac{\rho_x V_x}{\rho_o V_o}$$

across the duct for both methods is shown in Figures 23 and 24. The combustion efficiency based on the CO_2 was calculated to be 19.55 per cent and by the enthalpy method to be 24.95 per cent, showing a fairly close agreement. The enthalpy method is considered the more satisfactory, since enthalpy is the important parameter in propulsive systems.

This investigation indicates the slow rate of flame spreading behind the flameholder. At the station under investigation, which is approximately six ducts heights behind the flameholder, the burned zone occupies approximately one-third of the duct height and the fraction of fuel completely burned (η_c) is of the order of 25 per cent. If flame spreading were assumed linear with distance downstream of the duct, between 18 and 24 duct heights would be required for complete burning of the fuel mixture.

V. CONCLUSIONS

This investigation indicates that the methods of sampling and measurement, and the use of the Infra Red Analyzer are satisfactory for the analysis of the gas mixtures behind a flameholder. This investigation also shows the extreme importance of using the correct sampling rate.

The analysis of the combustion products and the investigation of the local mixture temperature and pressure profiles show that the flame is divided into the three distinct zones (unburned, reaction, and burned). The data indicate that a rapid change in composition occurs in the reaction zone and that the concentrations of important components are almost constant in the burned region. These data also indicate that the thickness of the reaction zone is large, about 16 per cent of the total duct height on each side of the flame, even at 34 1/8 inches behind the flameholder.

The experimental data suggest that for the purpose of analyzing the aerodynamic features of the flame spreading process, the reaction zone may be characterized by the following approximations without appreciable error: the temperature, density, and the mass flow per unit area (ρV) vary linearly through the reaction zone and are roughly constant in the burned zone; and the velocity may be approximated as a linear function from the outer edge of the reaction zone to the centerline.

Investigation of the CO concentration across the duct reveals the CO concentration is still high in the burned zone, which again indicates the slowness of the terminal steps in the hydrocarbon oxidation process.

The carbon balance across the duct is in agreement with the theoretical predictions, provided that proper allowance is made for the water vapor losses in the sample entering the analyzer. The excess carbon atoms in the reaction zone and the deficit of carbon atoms in the burned zone suggests that there is diffusion of CO_2 from the burned region, where CO_2 concentration is high, to the reaction zone, where the CO_2 concentration is relatively low. However, this suggested diffusion process is not important in fixing the overall carbon balance, and the accuracy of the methods used in this investigation is not high enough to show with condifence that diffusion actually occurs.

Flame spreading behind the flameholder is a slow process. In this work, the station investigated was approximately 6 duct heights behind the flameholder; yet the burned zone at this station occupied less than one-third of the duct height and the fraction of the fuel mixture completely burned (η_c) was 25 per cent. If the flame spreading in the duct were assumed linear with respect to distance downstream of the flameholder, as suggested in reference 7, it would take 18 to 24 duct heights for complete flame spreading and for complete combustion of the fuel mixture entering the duct.

REFERENCES

1. Nicholson, H. M. and Fields, J. P.: "Some Experimental Techniques to Investigate the Mechanism of Flame Stabilization in the Wake of Bluff Bodies," Part I. Third Symposium on Combustion, Flame, and Explosion Phenomena, Baltimore, Williams and Wilkins Company, (1949), pp. 44-68.

2. Longwell, J. P., Cheveny, J. E., Clark, W. W. and Frost, E. E. "Flame Stabilization by Baffles in a High Velocity Gas Stream," Part I. Third Symposium on Combustion, Flame, and Explosion Phenomena, Baltimore, Williams and Wilkins Company, (1949), pp. 40-41.

3. Haddock, G. W.: "Flame-Blowoff Studies of Cylindrical Flameholders in Channeled Flow", Progress Report No. 3-24, Pasadena, Jet Propulsion Laboratory, (May 14, 1951).

4. Scurlock, A. C.: "Flame Stabilization and Propagation in High Velocity Gas Streams," Meteor Report No. 19, Cambridge, Massachusetts Institute of Technology, (May, 1948).

5. Scurlock, A. C.: "Flame Stabilization and Propagation in High Velocity Gas Streams, Part I", Third Symposium on Combustion, Flame, and Explosion Phenomena, Baltimore, Williams and Wilkins Company, (1949).

6. Zukoski, E. E.; "Flame Stabilization on Bluff Bodies at Low and Intermediate Reynolds Numbers," Thesis, California Institute of Technology, Pasadena, (June, 1954).

7. Thurston, D. W.: "An Experimental Investigation of Flame Spreading from Bluff Body Flameholders," Thesis, California Institute of Technology, Pasadena, (June, 1958).

8. Satre, R. S.: "An Experimental Investigation of Flame Propagation Downstream of a Cylindrical Flameholder," Thesis, California Institute of Technology, Pasadena, California, (June, 1959).

9. Barbor, R. P., Larkin, J. D., Von Rosenberg, H. E.: "The Study of Flow and Reaction Rates in Turbulent Flames," American Institute of Chemical Engineers' Journal, (March, 1959).

10. Leeper, C. K.: "Sampling of Unmixed Gaseous Streams," Thesis, Massachusetts Institute of Technology, Cambridge, Massachusetts, (June, 1954).

11. Wright, F. H.: "Properties of Burned and Unburned Combustion Mixtures," Unpublished, Jet Propulsion Laboratory, Pasadena.

12. Scadron, M. D., Warshawsky, I.: "Experimental Determination of Time Constants and Nusselt Numbers for Bare Wire Thermocouples in High Velocity Air Streams and Analytic Approximation of Conduction and Radiation Errors," N. A. C. A. Technical Note 2599, Cleveland, (1952).

TABLE A

PROPERTIES OF STANDARD OIL THINNER NO. 200

1. Heat of combustion, net		18,675 BTU/lb
2. Average molecular weight		96
3. Latent heat of vaporization at 77°F		148 BTU/lb
Vapor pressure at 100°F		2.5 psi
4. Density, specific, at 60°F	0.	0.7366
Density, lb/gal, at 60°F		6.132 lb/gal
5. Hydrocarbon type analysis	Saturates	94.5%
	Olefins	00.5%
	Aromatics	05.0%

6. Distillation Astm

Initial	172°F
5	179
10	180
20	183
30	186
40	188
50	191
60	195
70	198
80	202
90	208
95	214
Dry	224

7. Chemical analysis (proportions by weight)

Carbon - 85.4% Hydrogen - 14.6%

8. Equivalent chemical formula - $C_{6.822}H_{13.955}$

TABLE B

TEMPERATURE EFFECT ON SAMPLE EXTRACTION RATE AT 1.4 IN. ABOVE CENTERLINE

TEMPERATURE °K	DENSITY lbs/cu ft	VELOCITY ft/sec	SAMPLE RATE gms/sec	CARBON CONCENTRATION gms C/gms C in Mixture			TOTAL CARBON CONCENTRATION	°/o ERROR
				CO_2	CO	CH		
25°/o Low 1228	.01775	550	.0609	.335	.098	.683	1.116	0.01
Normal 1635	.01330	635	.0527	.315	.093	.709	1.117	0.00
25°/o High 2042	.01068	707	.0471	.300	.091	.735	1.126	0.80

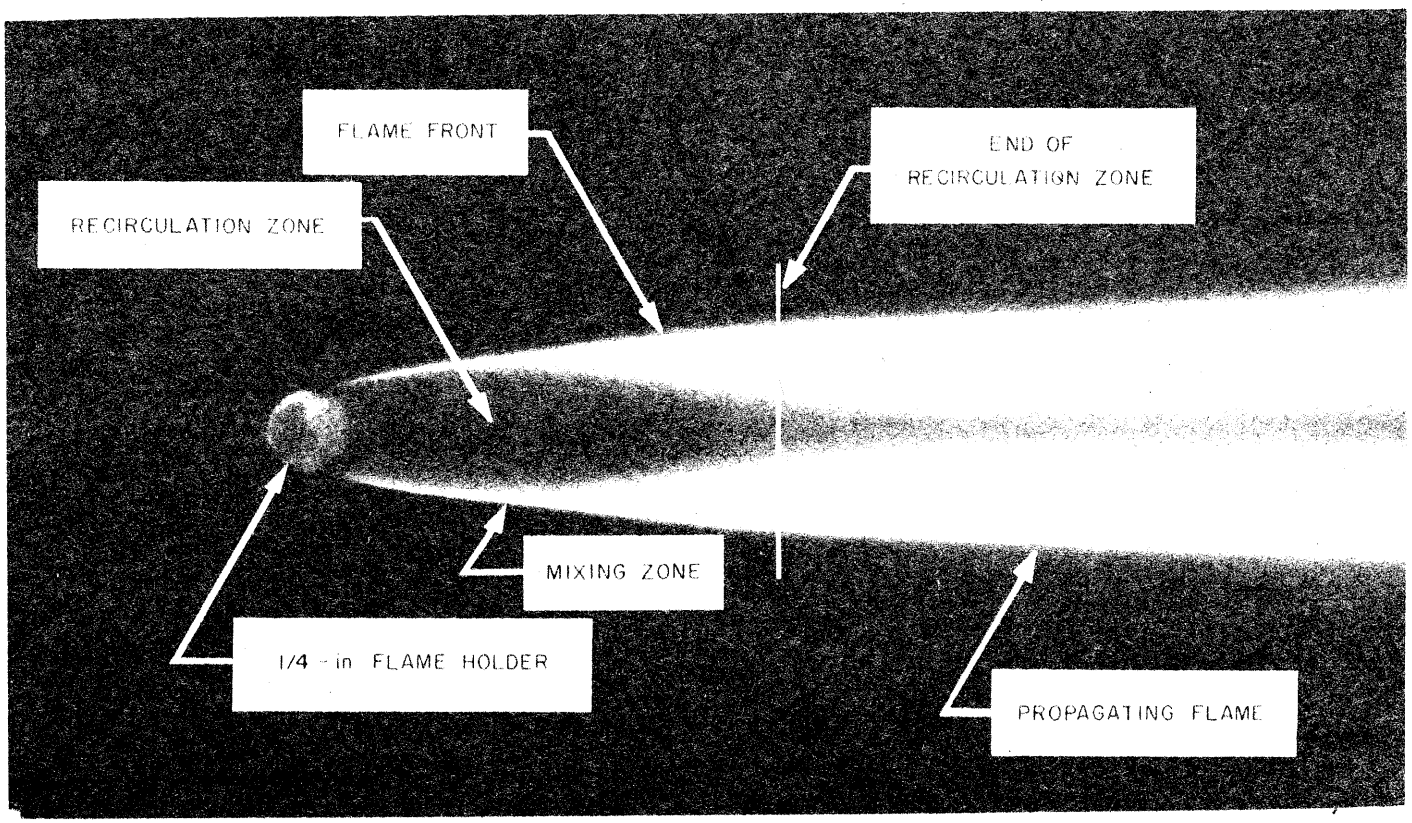

Fig. 1. Time Exposure of a Flame Stabilized on a 1/4 In. Diameter Flameholder

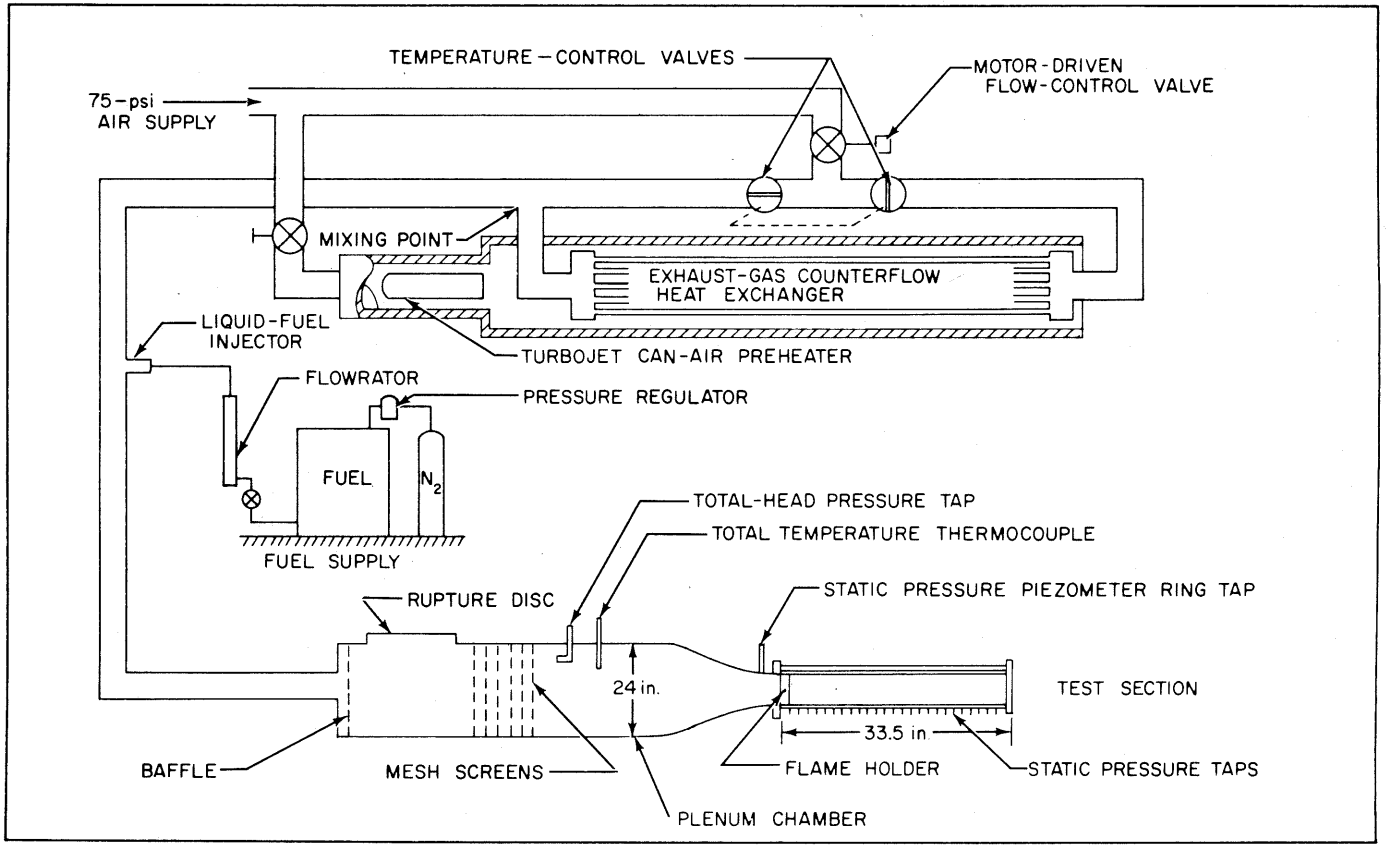

Fig. 2. Schematic Diagram of Flow System

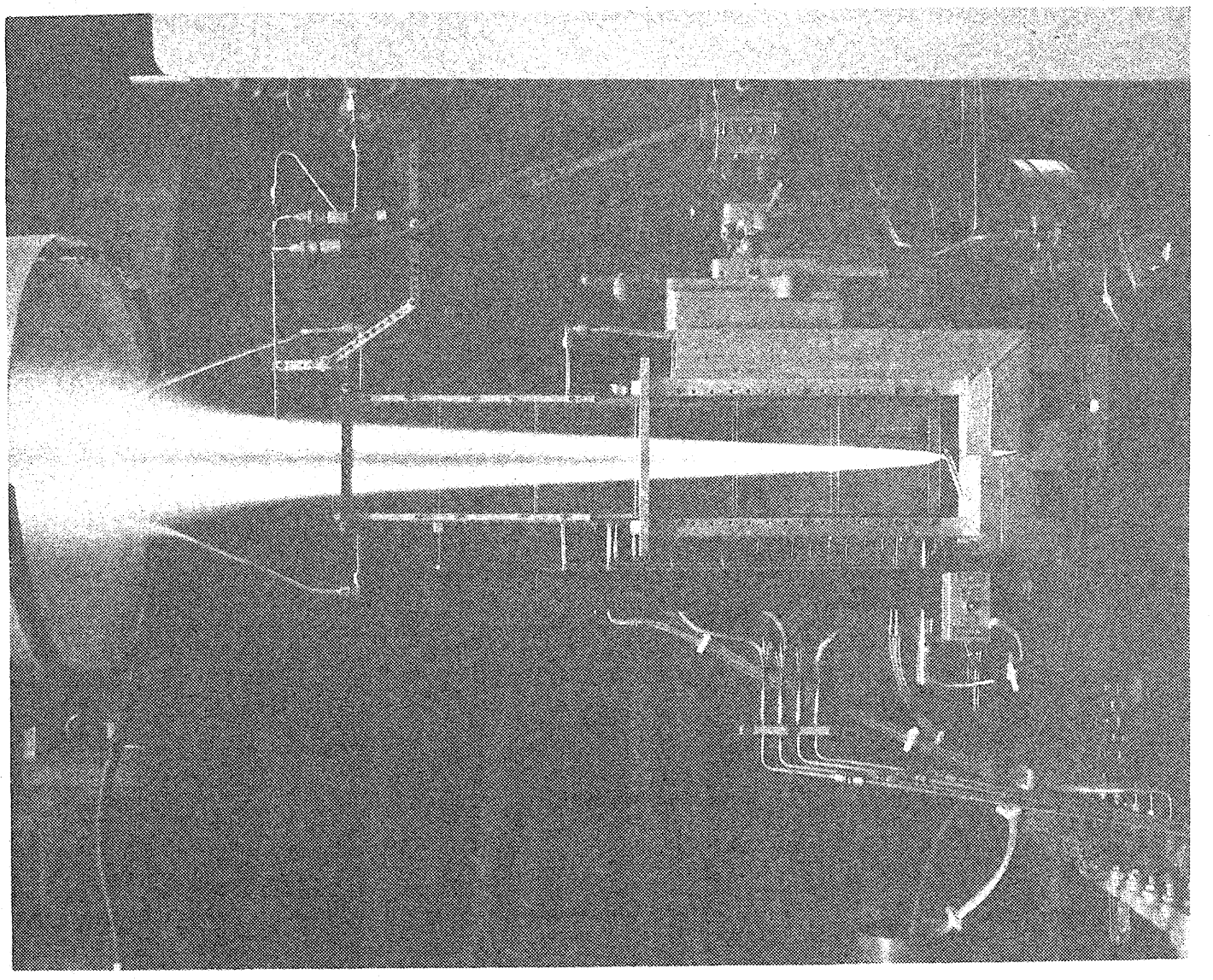

Fig. 3. Side View of Combustion Chamber with Flame Stabilized on a 1/4 In. Flameholder

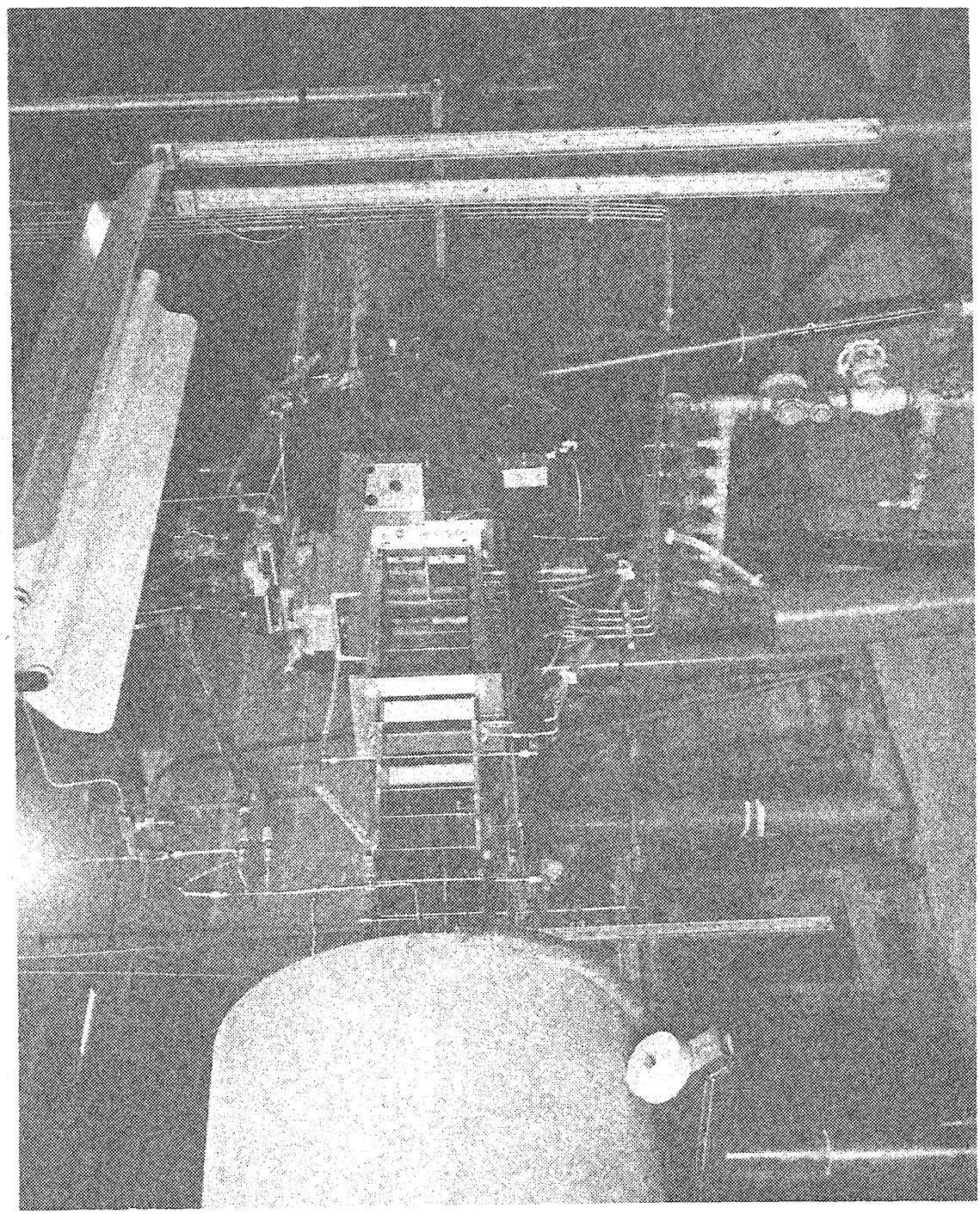

Fig. 4. Side View of Combustion Duct, Plenum Chamber, Nozzle, and Exhaust Tube.

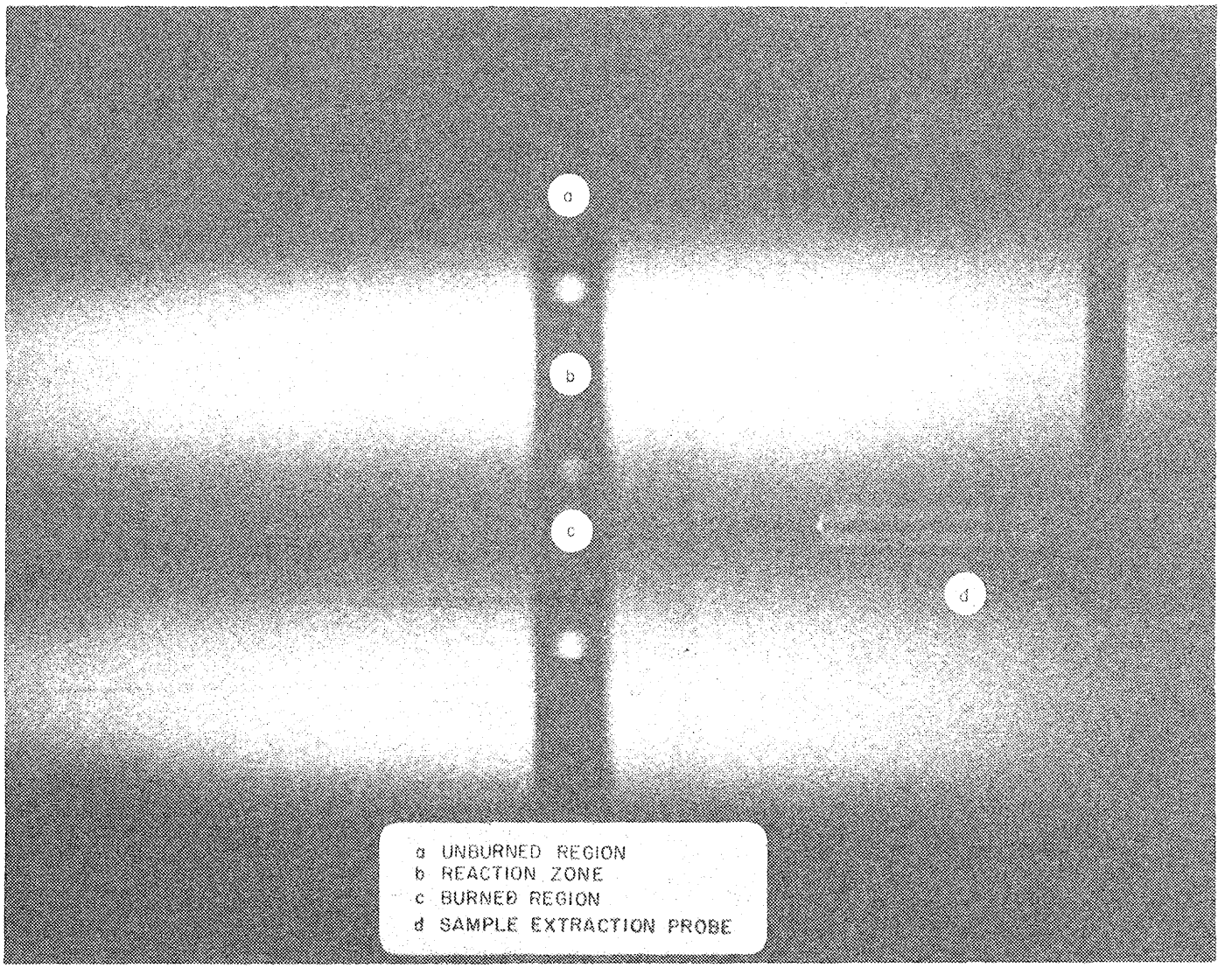

Fig. 5. Time Exposure of Flame Showing Three Distinct Zones. Station 34 1/8 In. $\phi = .93$.

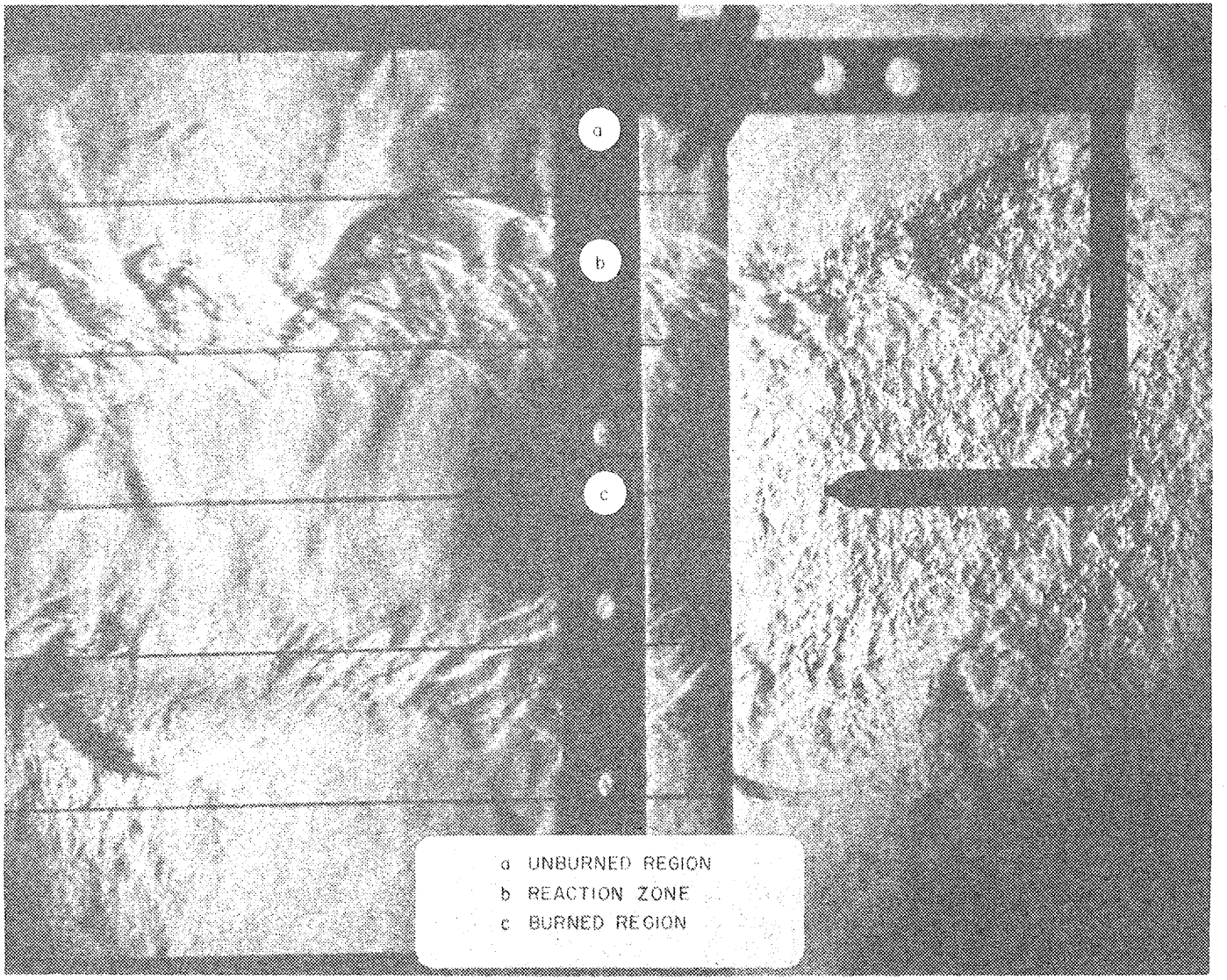

Fig. 6. Schlieren Photograph Showing the Three Distinct Zones in the Duct. Station 34 1/8 In., $\phi = .93$

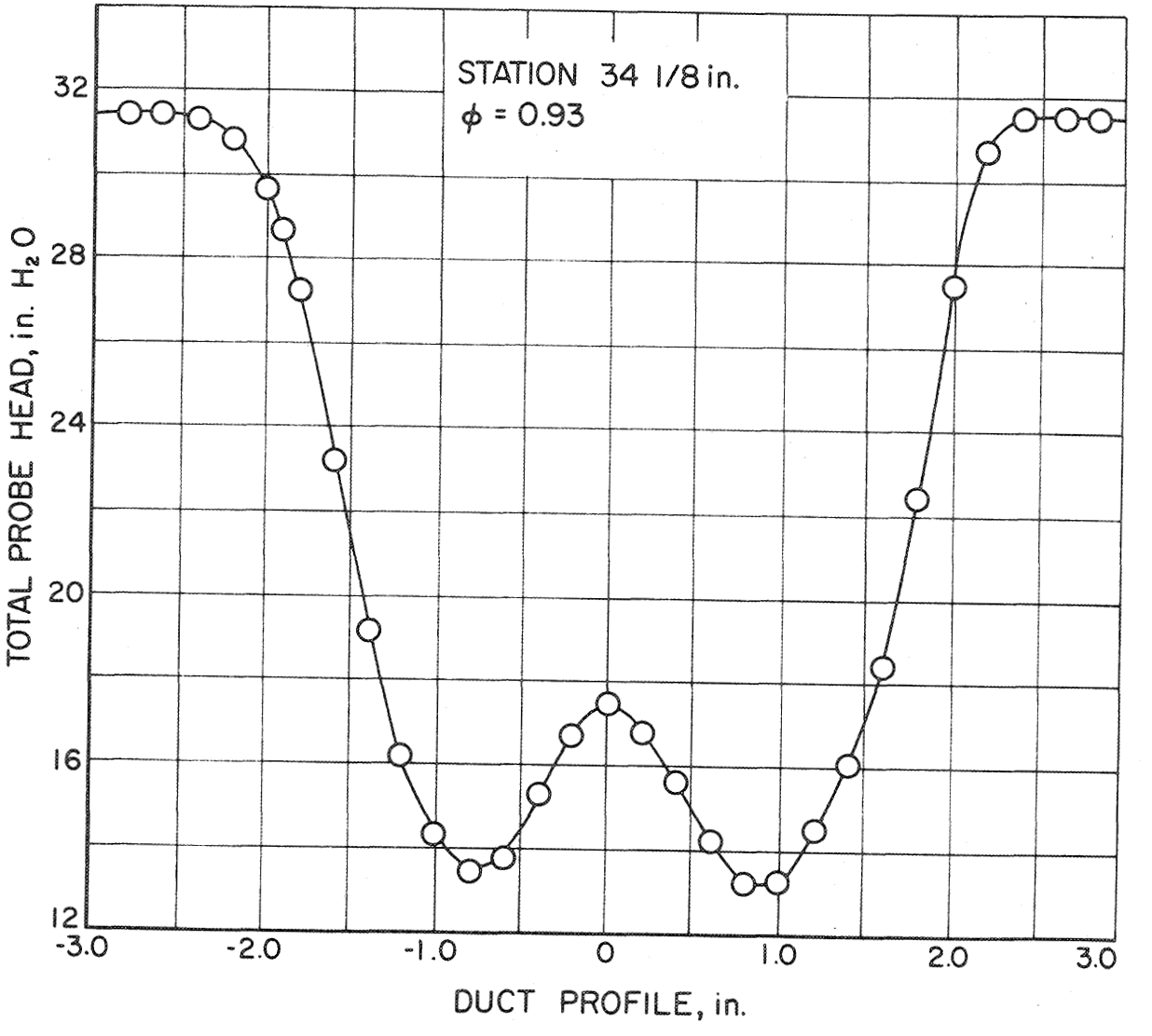

Fig. 7. Sample Probe Total Head Pressure Survey.

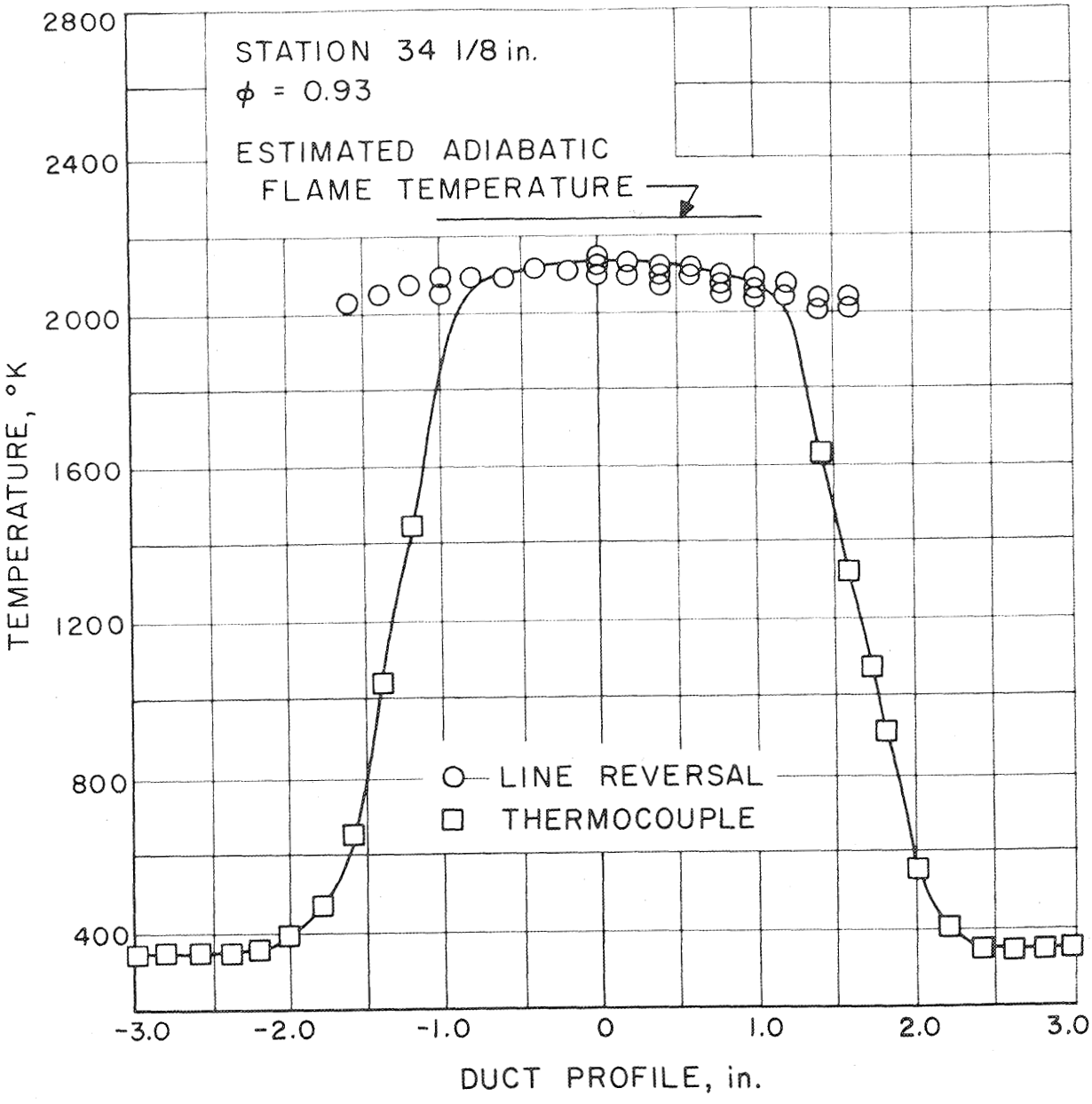

Fig. 8. Temperature Distribution.

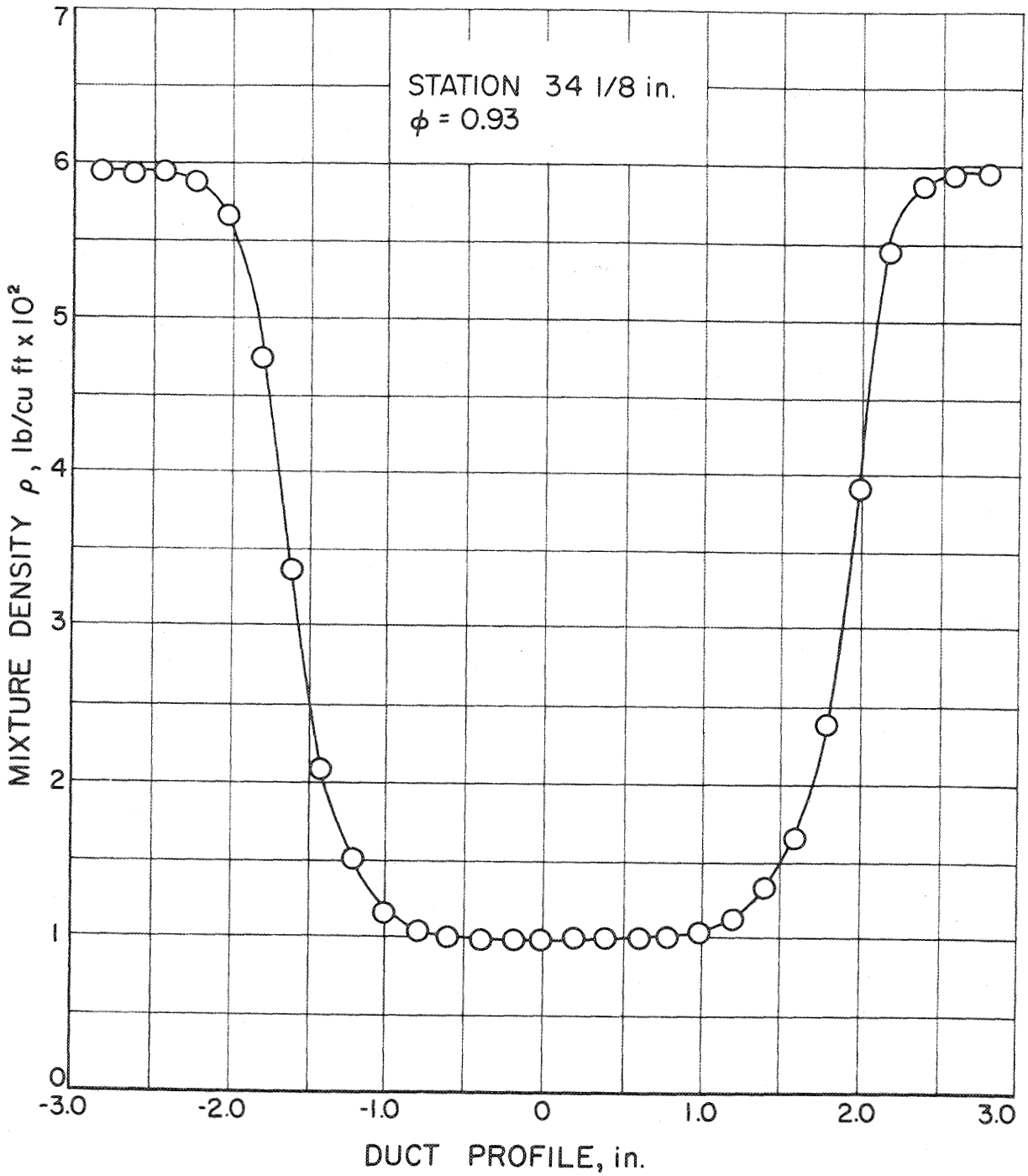

Fig. 9. Gas Density Survey.

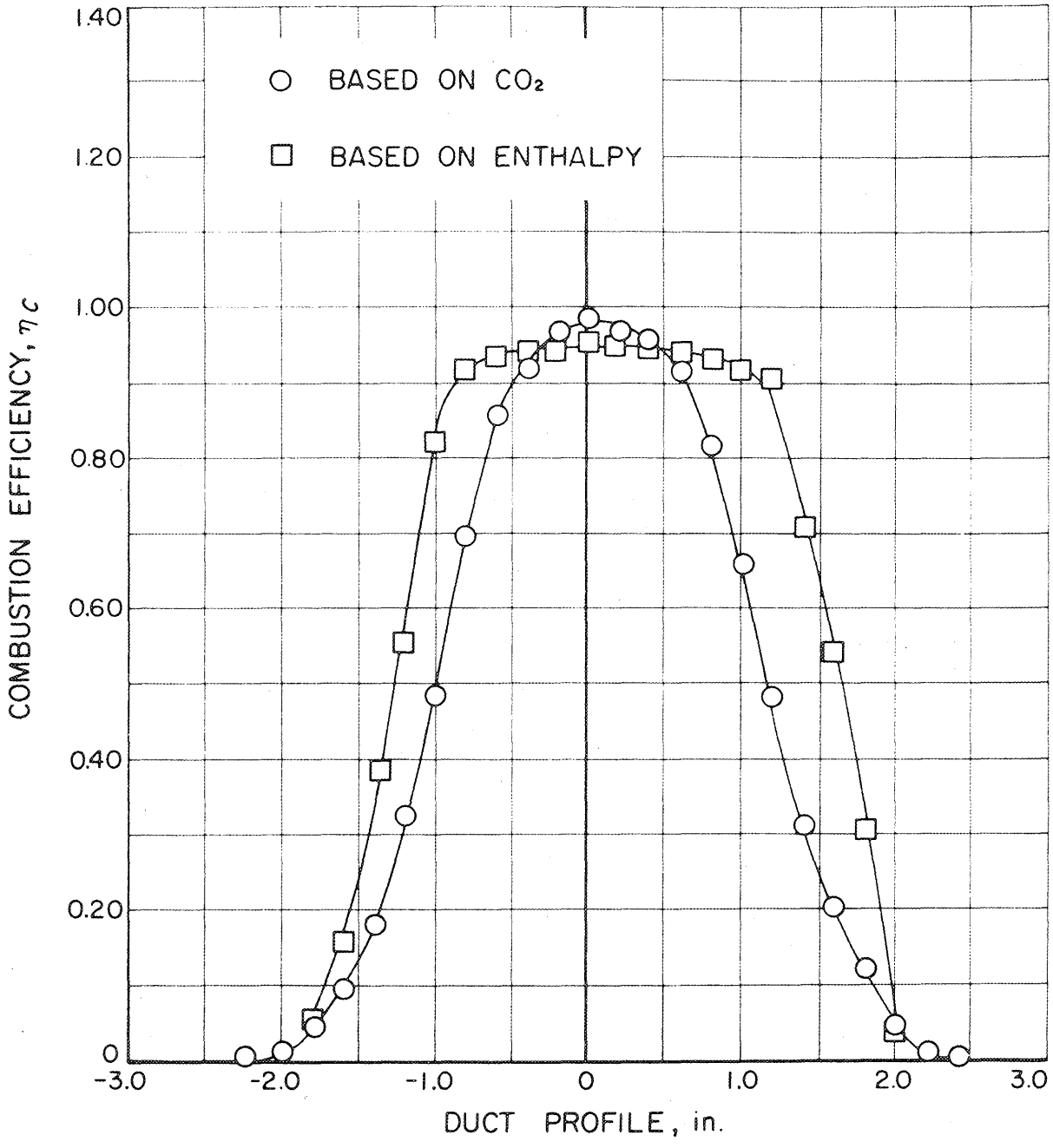

Fig. 10. Local Combustion Efficiency Distribution.

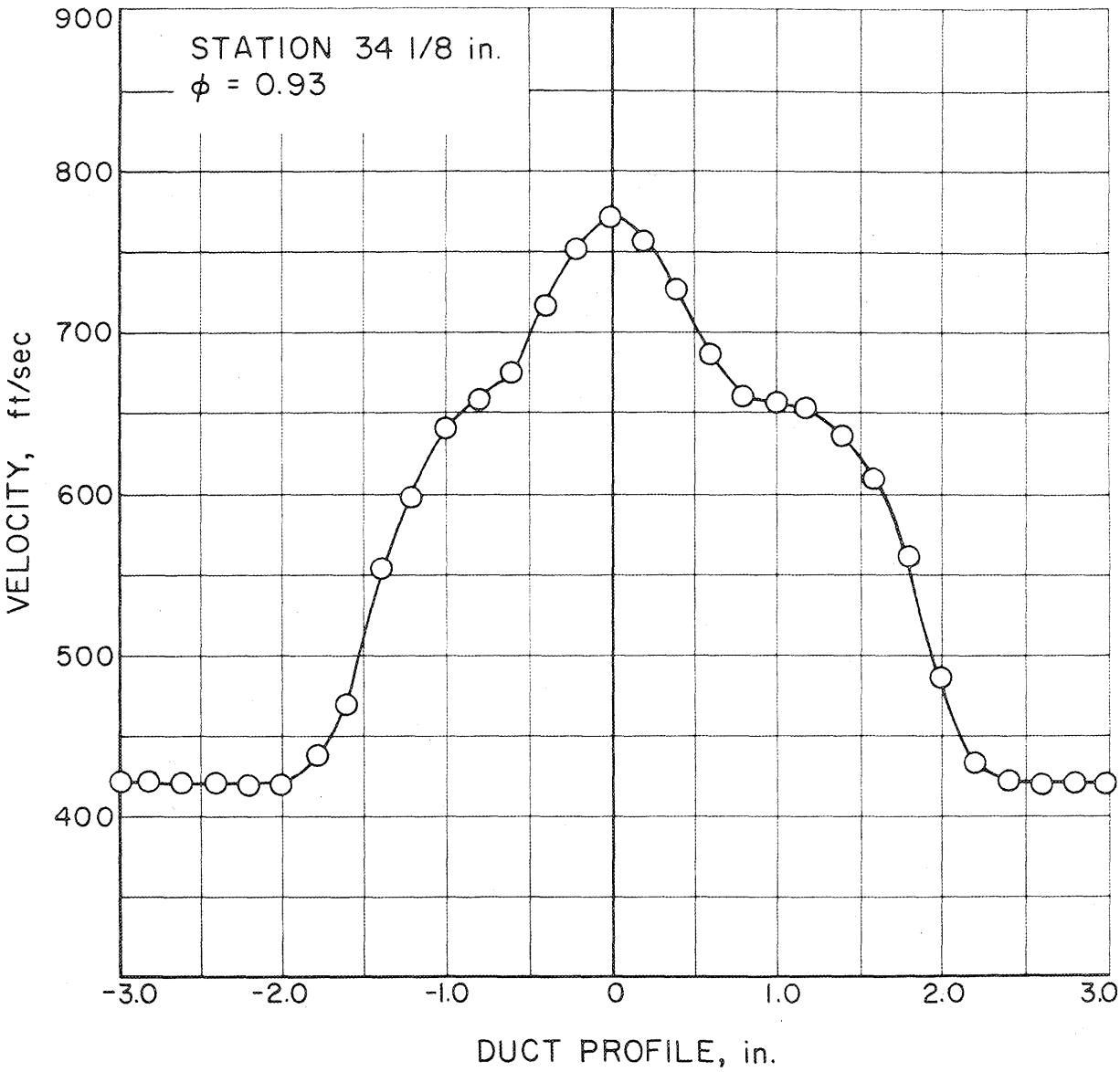

Fig. 11. Gas Velocity Distribution.

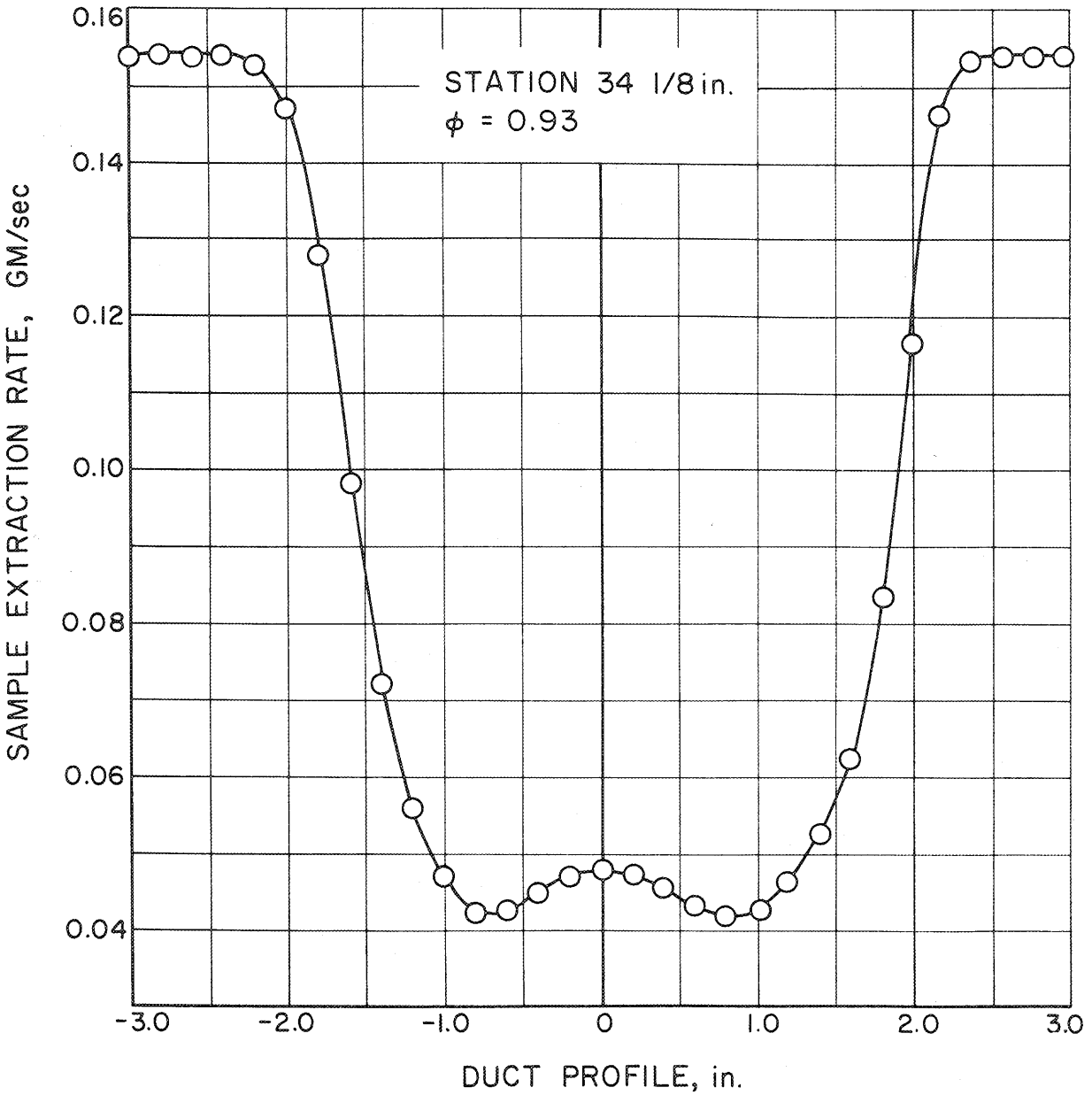

Fig. 12. Sample Flow Rate Distribution.

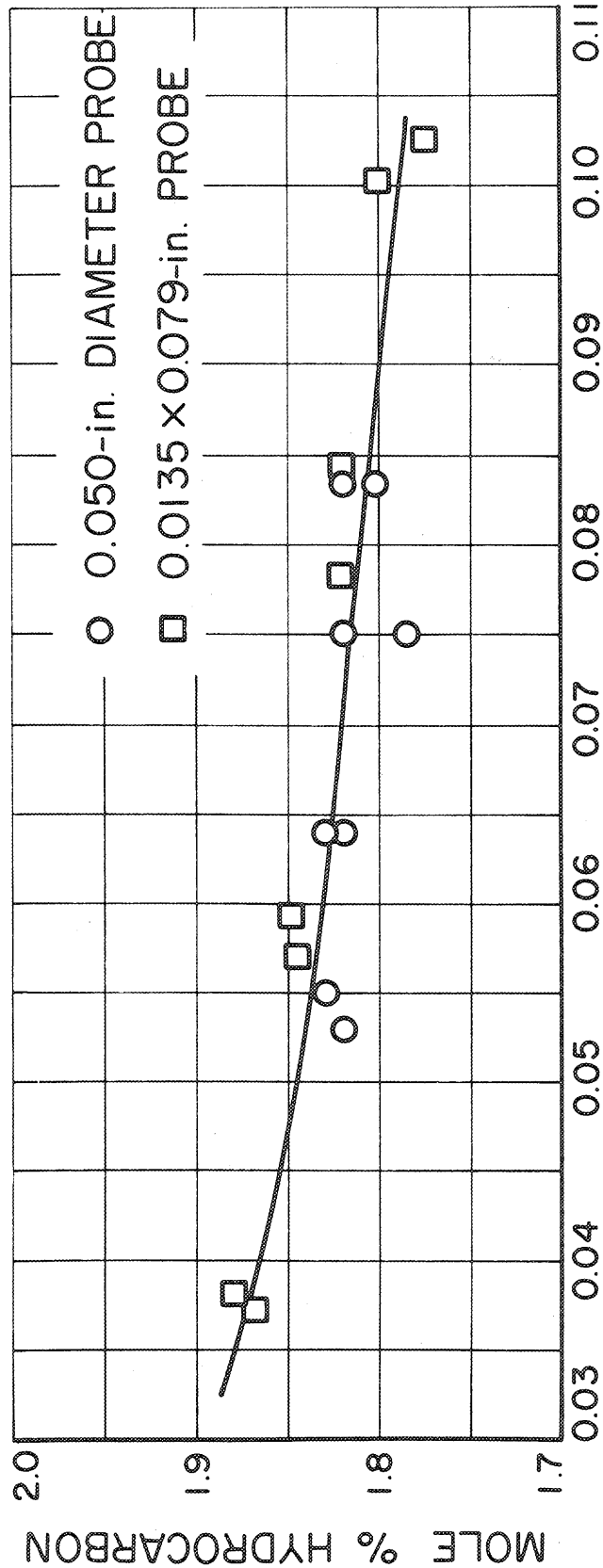

Fig. 13. Variation of Sample Concentration with Sample Probe Size. Station 1.6 In. Below Centerline.

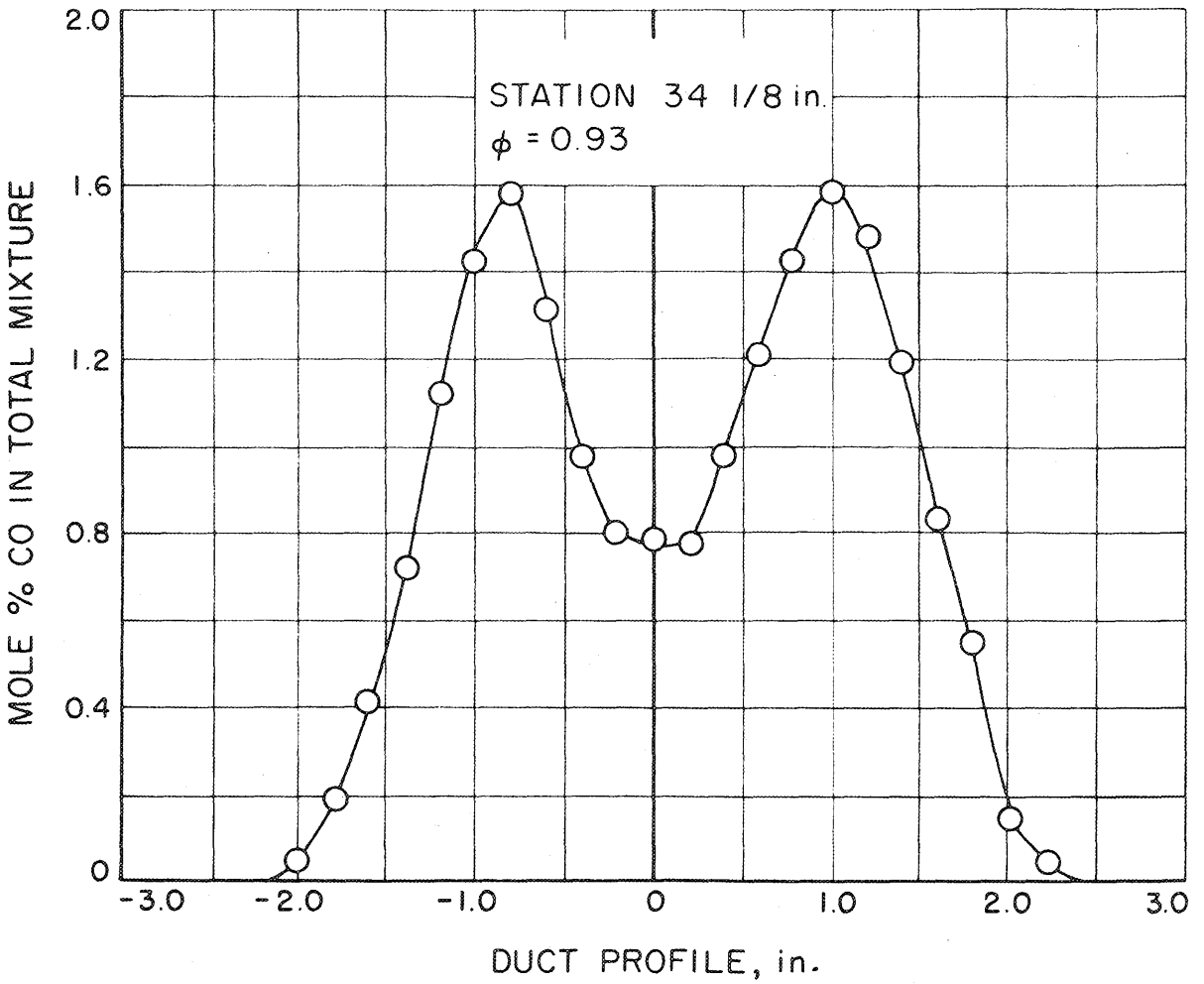

Fig. 14. CO Distribution.

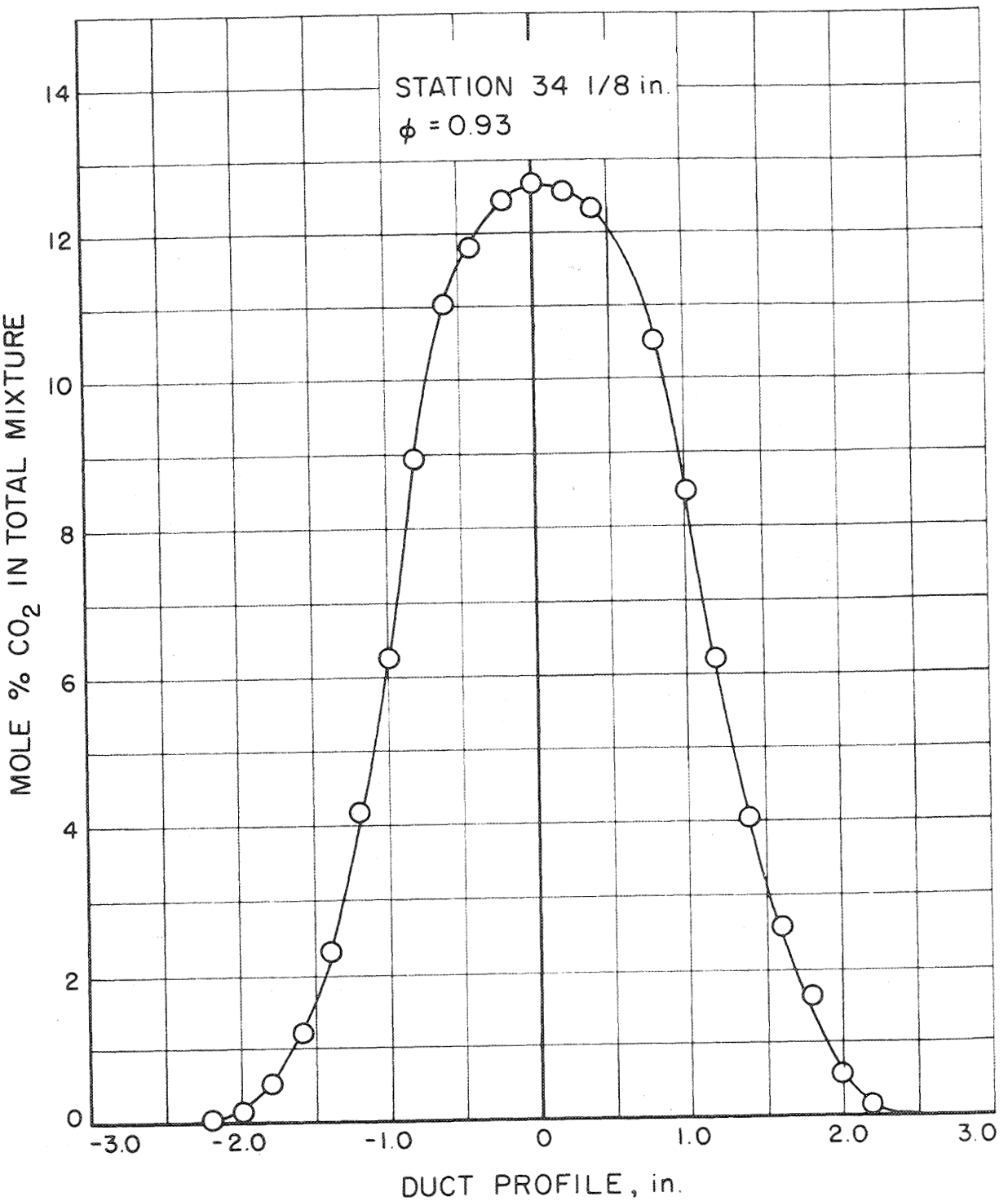

Fig. 15. CO_2 Distribution.

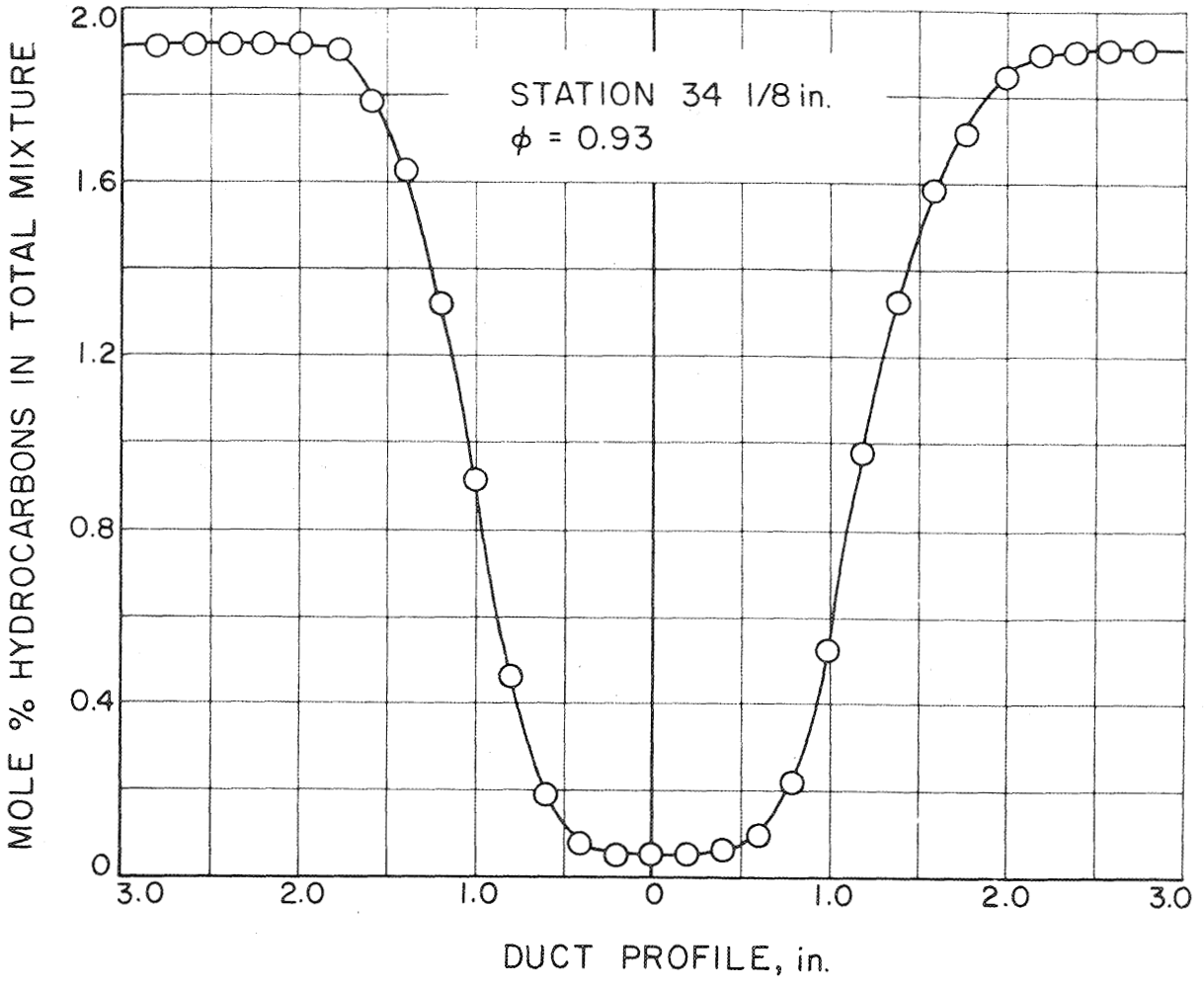

Fig. 16. Hydrocarbon Distribution Across the Duct.

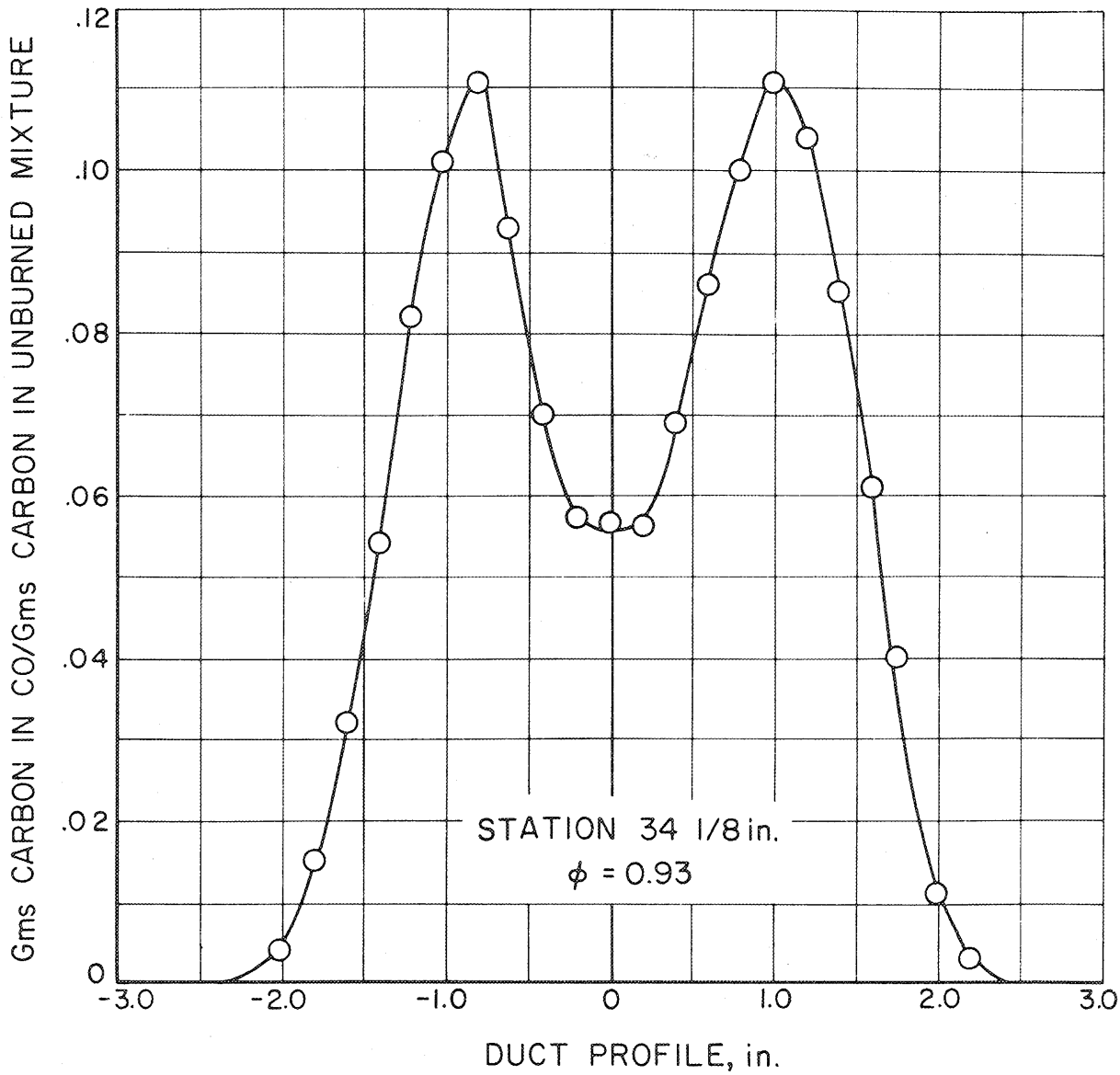

Fig. 17. Normalized CO Concentration Based on Dry Sample.

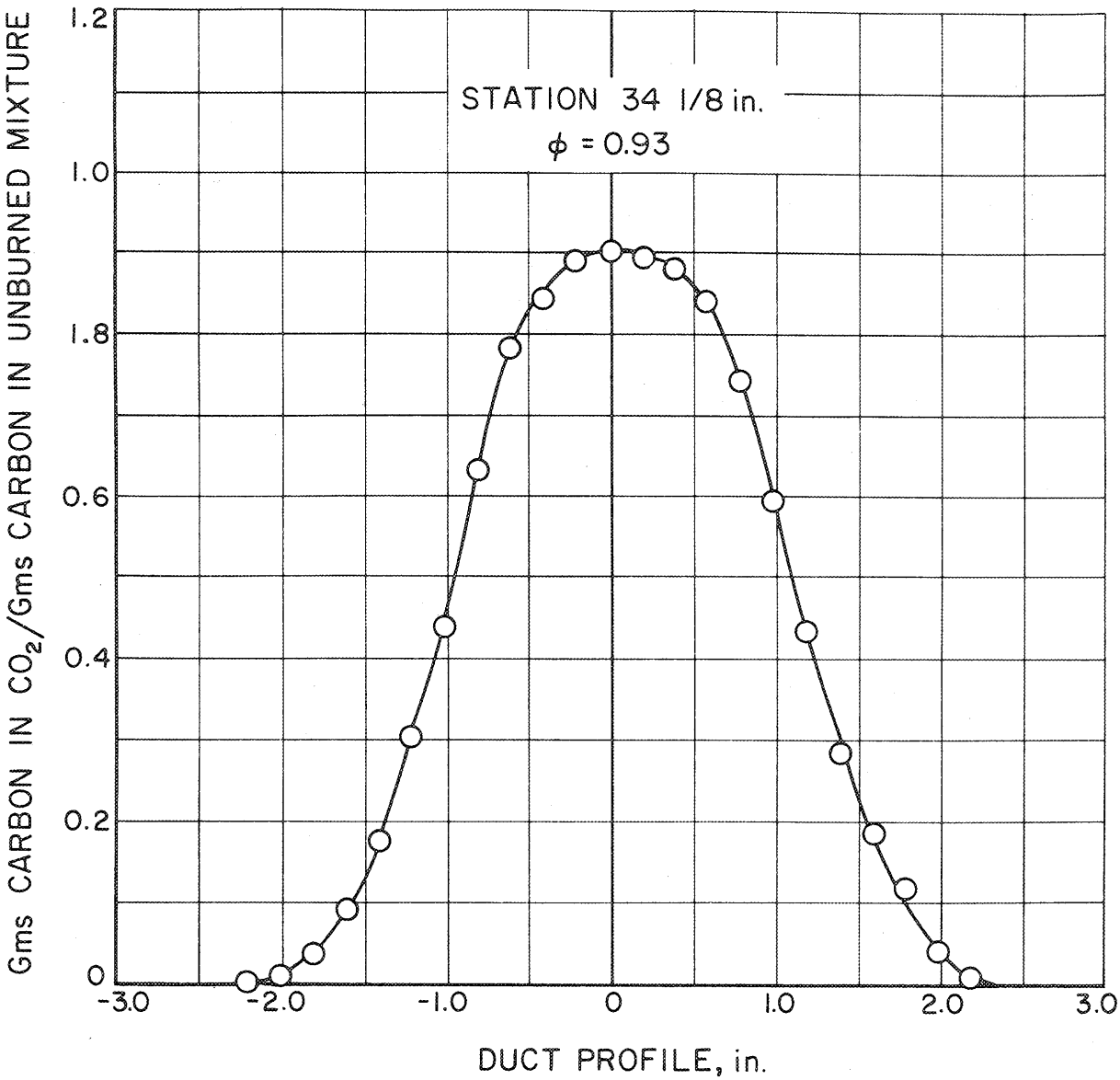

Fig. 18. Normalized CO_2 Concentration Based on Dry Sample.

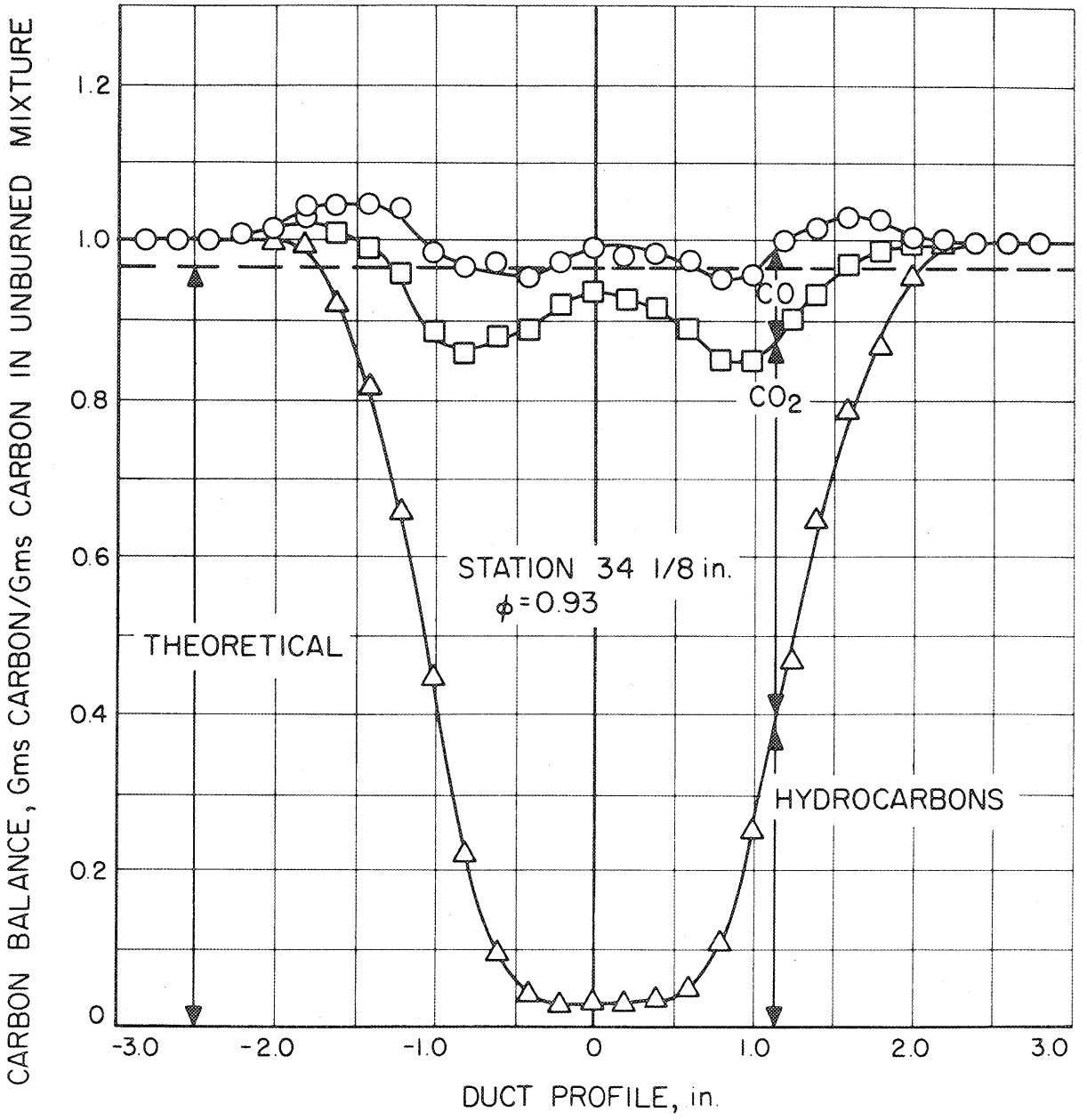

Fig. 19. Carbon Balance Across the Duct Based on Dry Sample.

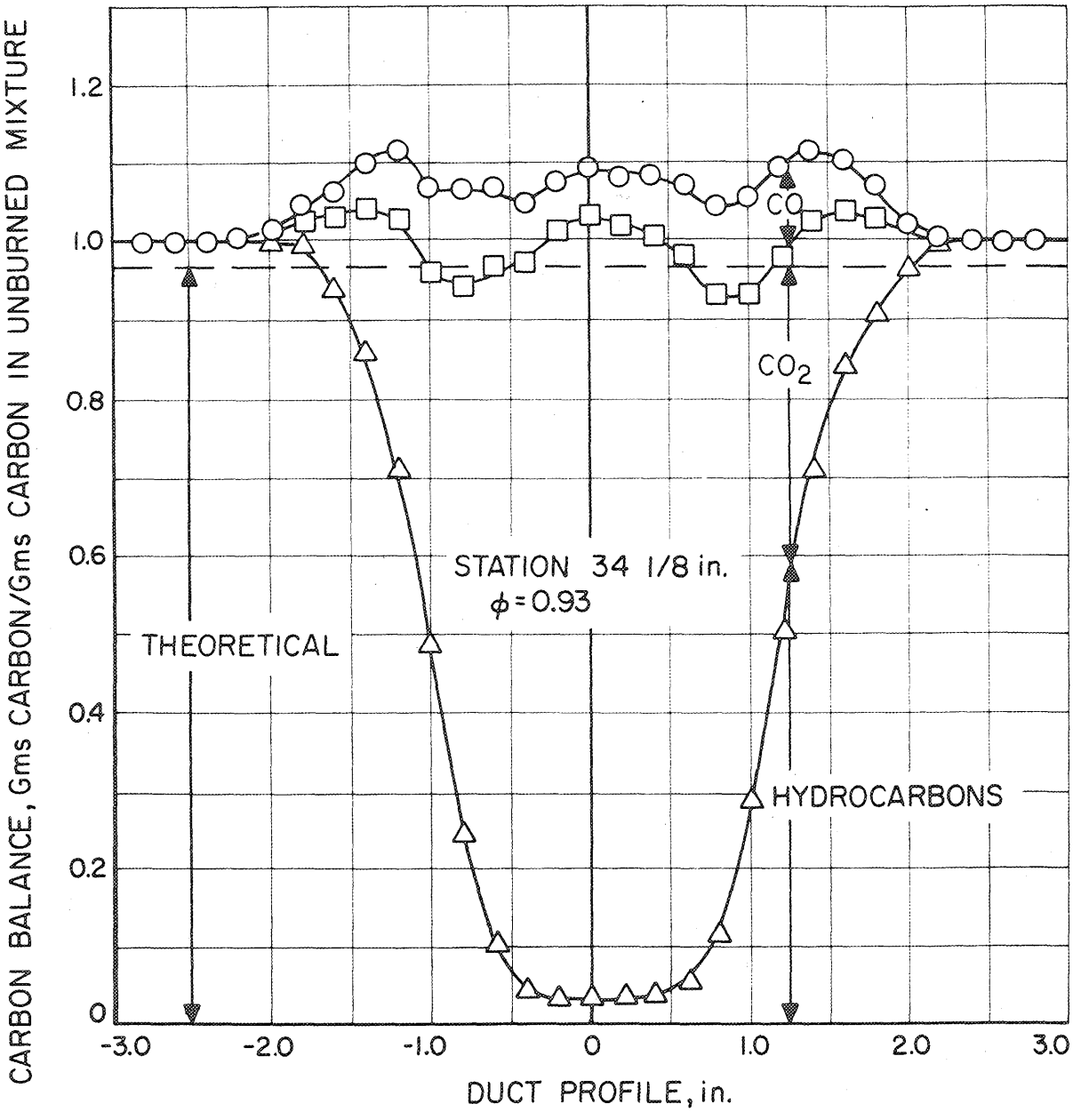

Fig. 20. Carbon Balance Across the Duct Based on Saturated Sample.

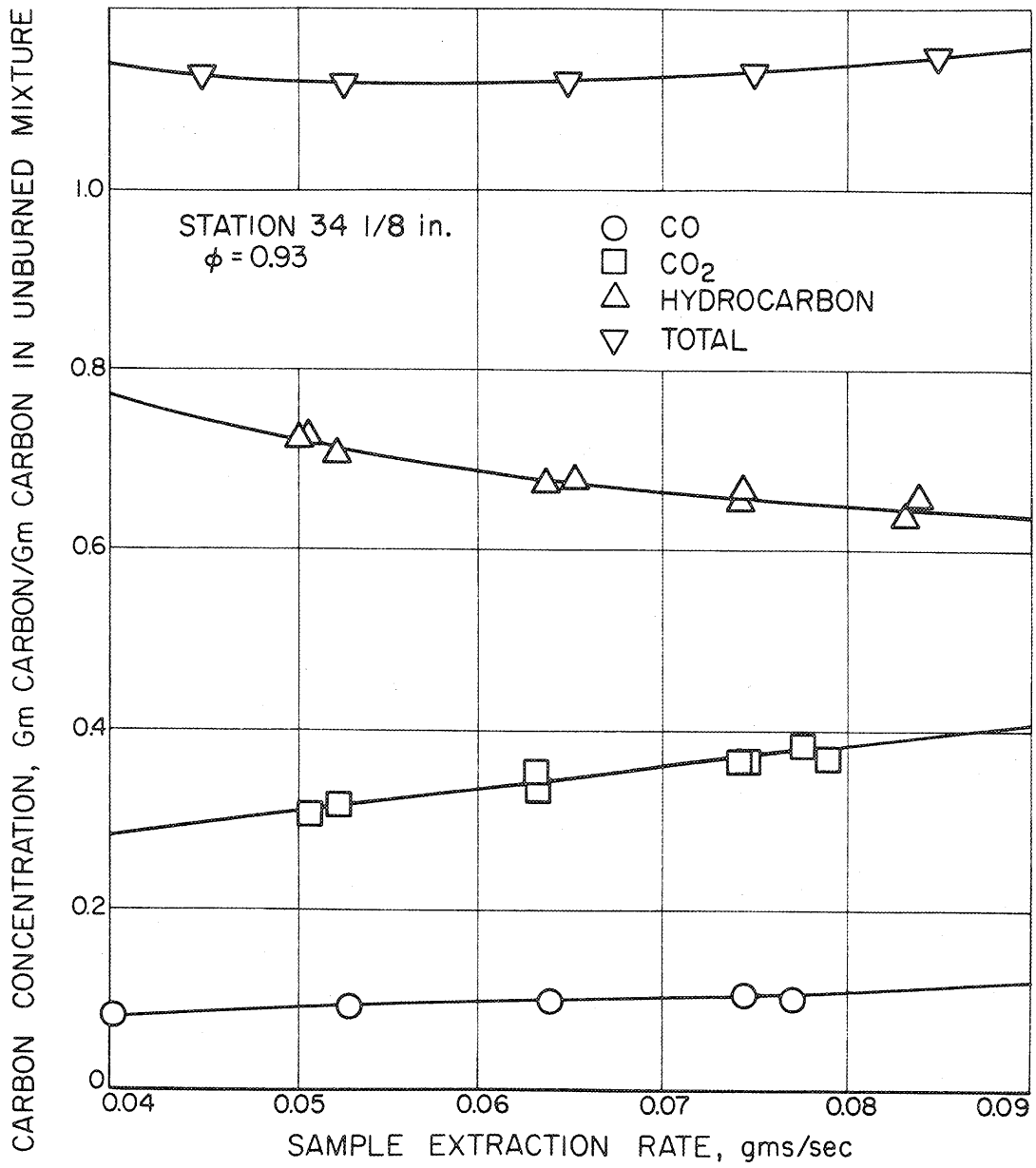

Fig. 21. Carbon Concentration Vs Sampling Rate 1.4 In. Above Centerline.

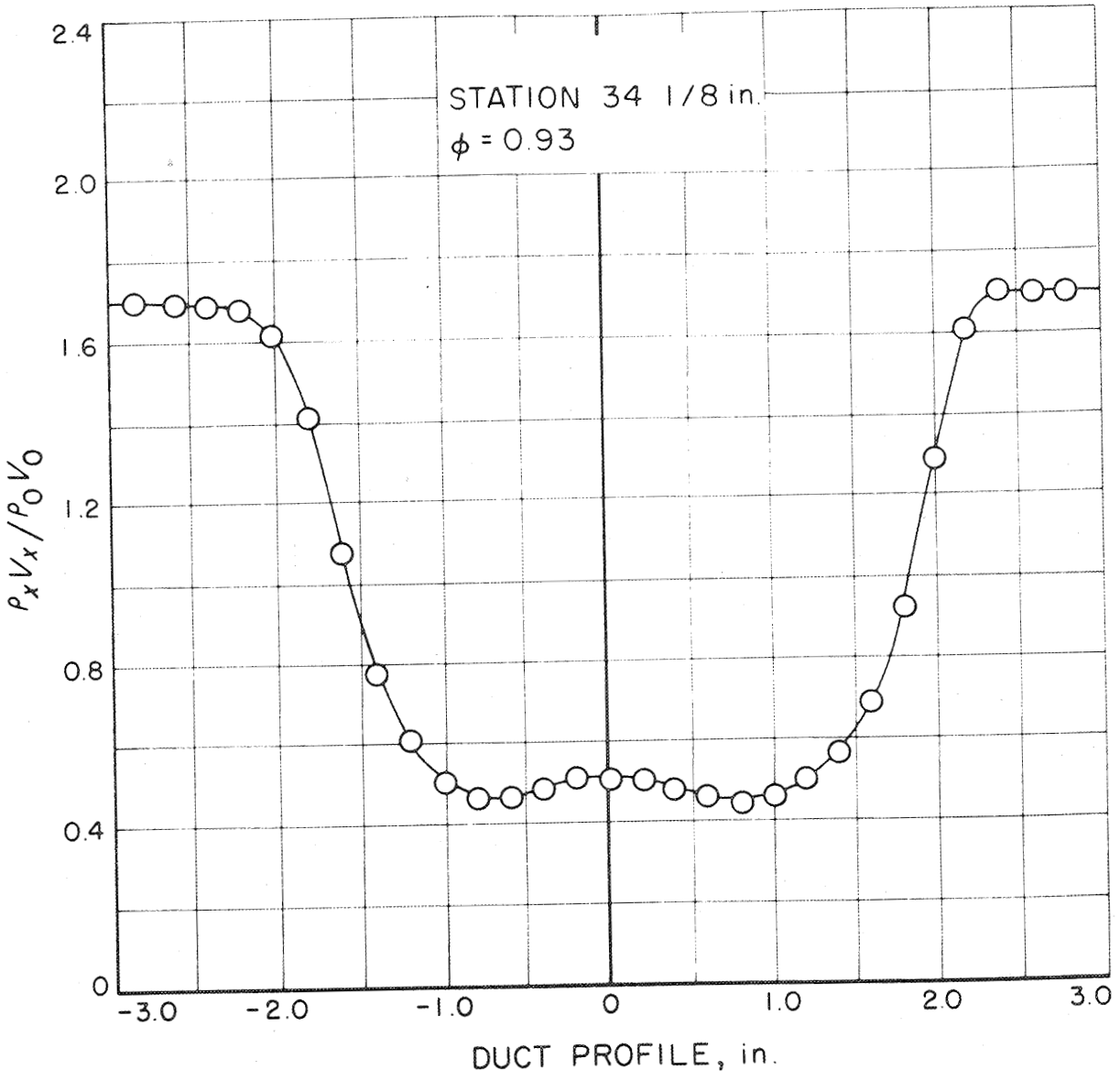

Fig. 22. $\rho_x V_x / \rho_o V_o$ Distribution.

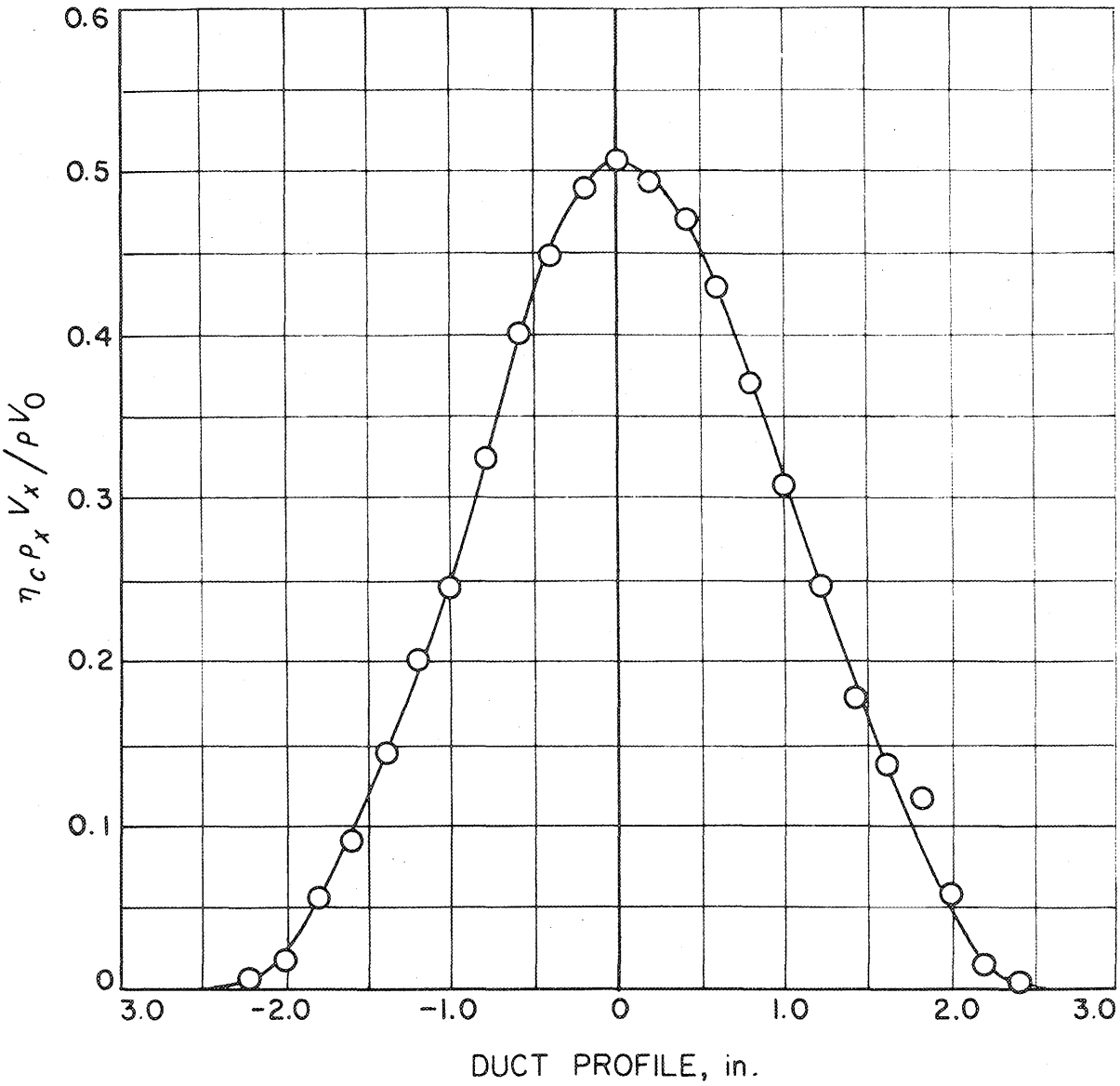

Fig. 23. Distribution of Combustion Efficiency Parameter Based on CO_2.

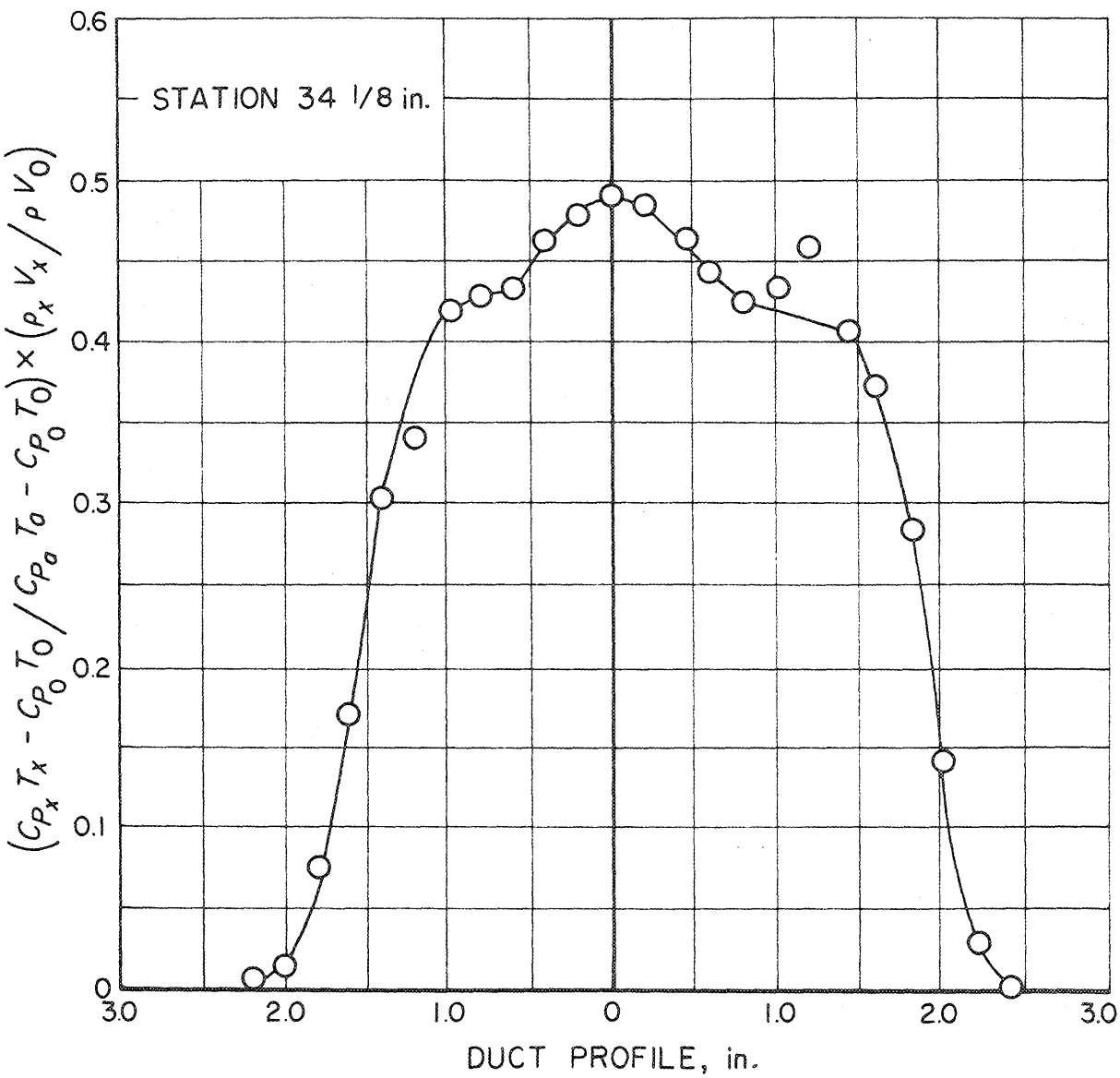

Fig. 24. Distribution of Combustion Efficiency Parameter Based on Enthalpy